Free vibration analysis of sandwich plates with compressible core in contact with fluid

Arash Ramian[1], Ramazan-Ali Jafari-Talookolaei[1*], Paolo S. Valvo[2], Maryam Abedi[3]

[1] School of Mechanical Engineering, Babol Noshirvani University of Technology, Shariati Av., 47148-71167, Babol, Mazandaran, Iran.
[2] Department of Civil and Industrial Engineering, University of Pisa, Largo Lucio Lazzarino, I-56122 Pisa, Italy.
[3] Department of Mechanical Engineering, Faculty of Engineering and Technology, University of Mazandaran, Babolsar, Iran.
[*] Corresponding Author, Email: ramazanali@gmail.com, ra.jafari@nit.ac.ir

Abstract

In this paper, the extended higher-order sandwich plate's theory (EHSAPT) is used to analyze the free vibration of the sandwich plate with compressible core and different boundary conditions in contact with fluid. First-order shear deformation theory is adopted for the top and bottom face sheets, while the in-plane and transverse displacements of the core are considered to be cubic and quadratic functions of the transverse coordinate, respectively. A single series is considered with two-variable orthogonal polynomials as a set of admissible functions satisfying the boundary conditions. Besides, the fluid is considered to be irrotational, inviscid and incompressible. By taking into account the boundary conditions and compatibility conditions, the fluid velocity potential is acquired. The natural frequencies of the system are calculated by the Rayleigh-Ritz method. An excellent accuracy is obtained between the results in the available literature and the present method. Finally, the effects of various parameters including boundary conditions, side-to-thickness ratio, thickness of the core to thickness of the face sheets ratio, face sheet to core flexural modulus ratio, dimensions of the container, and aspect ratios on the natural frequencies of the sandwich plate are presented and discussed in detail.

Keywords: Free vibration; Fluid-sandwich plate interaction; Compressible core; Different boundary conditions; Two-variable orthogonal polynomials.

Nomenclature

a	Sandwich plate length
b	Sandwich plate width
c	Fluid width
d	Fluid depth
$f_i(x,y)$	Weight function
f_t	Top face sheet thickness
f_b	Bottom face sheet thickness
f_c	Core thickness
g	Acceleration of gravity
h	Sandwich plate thickness
$i=\sqrt{-1}$	Imaginary unit
$I^{t,b,c}$	Inertia terms of the face sheets and core
k_s	Shear correction factor

M	Number of terms in displacement and rotation series
M_1, N_1	Number of terms in fluid series
T_{fB}	Fluid kinetic energy related to bulging modes
T_{fS}	Fluid kinetic energy related to sloshing modes
$T_{t,b,c}$	Kinetic energy of the face sheets and the core
t	Time
$U_{t,b,c}$	Strain energy of the face sheets and the core
$u_0^{t,b}$	In-plane displacement of the face sheets along *x*-axis
$u_{0,1,2,3}$	Components of in-plane displacement of the core along *x*-axis
$v_0^{t,b}$	In-plane displacement of the face sheets along *y*-axis
$v_{0,1,2,3}$	Components of in -plane displacement of the core along *y*-axis
$w_0^{t,b}$	Transverse displacement of the face sheets
$w_{0,1,2}$	Transverse displacement of the core
$\rho_{t,b,c}$	Density of the face sheets and the core
ρ_f	Density of fluid
Φ_O	Fluid velocity potential
Φ_B	Fluid velocity potential associated with bulging modes
Φ_S	Fluid velocity potential associated with sloshing modes
x, y, z	Coordinates of system
$\psi_x^{t,b}$	Rotation component of the transverse normal along *y*-axis
$\psi_y^{t,b}$	Rotation component of the transverse normal along *x*-axis
ε	Strain field
σ	Stress field
ω	Dimensionless natural frequency
$\bar{\omega}$	Natural frequency
λ^k	Member of orthogonal polynomials
Λ_{lk}	Fourier coefficients related to the bulging modes
Γ_{ij}	Fourier coefficients related to the sloshing modes
∇^2	Laplace operator

Abbreviation

Extended higher-order sandwich plate's theory	EHSAPT
Two-dimensional	2D
Three-dimensional	3D
Equivalent single layer	ESL
Layer-wise	LW
Classical lamination theory	CLT
First-order shear deformation theory	FSDT
Functionally graded materials	FGM
Higher-order sandwich plate theory	HSAPT
Fluid-structure interaction	FSI
Simply-supported	S
Clamped	C
Free	F

Finite Element Method	FEM

1. Introduction

Sandwich structures with laminated composite face sheets and honeycomb or foam cores are being used increasingly in various industrial areas including aerospace, automotive, locomotive, and mechanical engineering [1-4]. The most important advantage of this type of sandwich structures is their high strength-to-weight ratio [5]. Although, these structures are primarily built to operate under harsh environmental conditions, in particular high temperature applications and wet environments [6]. Honeycomb cores are usually regarded as incompressible which have high specific stiffness and strength, while foam cores are considered compressible with low specific stiffness and strength [7]. The behavior of the core has significant effects on the overall behavior of the sandwich structure.

Two main approaches are available to obtain the response of a sandwich plate, based on three-dimensional (3D) elasticity and two-dimensional (2D) structural theories. In turn, according to the assumptions for the displacement field, 2D models are classified into two categories: equivalent single layer (ESL) and layer-wise (LW) models.

In recent years, many studies have been conducted on sandwich plates with both compressible and incompressible cores. Pagano [8] has used 3D elasticity solutions to solve the bending problem of simply-supported multilayered cross-ply plates. Moreover, by using 3D elasticity approach, the buckling and free vibrations of simply-supported sandwich panels with composite face sheets have been studied by Noor et al. [9]. Srinivas et al. [10-12] have provided exact analytical solutions for the bending, vibration, and buckling of homogeneous and laminated thick rectangular plates.

In the ESL approach, the multilayered plate is reduced to a single equivalent layer thanks to the constitutive relations of plate theories. The simplest ESL models of sandwich structures are based on classical lamination theory (CLT) and first-order shear deformation theory (FSDT). It is worth mentioning that in ESL approach, the core will be modeled similar to the other layers located at the top and bottom face sheets. By using CLT and FSDT for sandwich structures with highly compressible cores, results may become inaccurate because the CLT ignores transverse shear deformation. Also, the accuracy of the FSDT depends strongly on the shear correction factor that modifies the through-the-thickness distribution of the transverse shear stresses. To solve the problem of the shear correction factor and calculating the real through-the-thickness distribution of transverse shear stresses, higher-order theories have been presented. Kant and Mallikarjuna [13], Kant and Swaminathan [14] and Swaminathan et al. [15, 16] have performed an analysis of the sandwich plate by using the higher-order theories. Furthermore, based on the higher-order theory, different finite element analyses have been carried out by Meunier and Shenoi [17] and Nayak [18]. Also, Bardell et al.[19] have provided an analysis of sandwich plates by using a zig-zag displacement pattern through the thickness.

Contrary to the ESL approaches, in LW models, each layer (top face sheet, bottom face sheet, and core) behaves as a separate plate and also their kinematic relations are expressed separately. Besides, the compatibility conditions allow the layers to bond together. The natural frequencies of simply-supported sandwich plates based on a LW model have been studied by Rao and Desai [20]. Frostig et al. [21] have developed the higher-order sandwich plate theory (HSAPT), whereas the core is assumed to be compressible and its in-plane rigidity is ignored. Two models have been developed. In the first model, the displacement fields of the top and bottom face sheets, as well as the transverse shear stresses of the core, are expanded using polynomials. In the second model, the displacement fields of the top and bottom face sheets and the core are represented as polynomials. Malekzadeh et al. [22] have used Navier's technique to present free vibrations of sandwich plates with flexible viscoelastic core and simply-supported boundary condition. Also, Malekzadeh et al. [23] have reported dynamic responses of sandwich plates with viscoelastic core and arbitrary boundary conditions by using double Fourier series functions and Stokes's transformation technique. Free vibration analysis of sandwich plates with functionally graded face sheets and temperature-dependent material properties has been presented by Khalili et al. [24]. Singh et al.[25] have performed a nonlinear analysis of the sandwich Functionally Graded Materials (FGM) on Pasternak foundation under thermal environment. Recently, Sayyad et al. [26] have presented a comprehensive review on the free vibrations of multilayered laminated composite and sandwich plates using various methods. It should be noted that HSAPT only considers the out-of-plane stresses of the core, while the in-plane stresses are ignored. By utilizing the extended higher-order sandwich plate theory (EHSAPT), both the in-plane and out-of-plane stresses of the core are considered. Another advantage of the EHSAPT model over the HSAPT model is that EHSAPT model contains high modes including vibrations along the depth of the core, which the HSAPT model cannot identify.

In recent years, the number of studies on fluid-structure interaction (FSI) has remarkably increased. It is obvious that the presence of a fluid changes the vibrational behavior of a plate. Therefore, the natural frequencies of the wet modes are changed and reduced compared to the dry modes. Zhou and Cheung [27] have used the Rayleigh-Ritz method to study the vibrations of a rectangular plate in contact with a fluid. By applying the boundary element method, the natural frequencies of cantilever plates partially submerged in fluid have been obtained by Ergin and Ugurlu [28]. Chang and Liu [29] have carried out the free vibration analysis of rectangular plates with different boundary conditions interacting with a fluid. Khorshidi and Farhadi [30] have studied the free vibration analysis of a laminated composite rectangular plate in contact with a fluid by employing the Rayleigh-Ritz method. Furthermore, Cheung and Zhou [31] have used the Ritz approach to investigate the dynamic characteristics of the fluid-structure interaction of the rectangular plate. Besides, these authors [32] have employed the Galerkin method to investigate the free vibration of a circular plate coupled with the fluid. Omiddezyani et al. [33] have investigated the size-dependent free vibration analysis of a rectangular microplate coupled with fluid.Ugurlu et al. [34] have developed mixed-type finite element formulation and a boundary element approach to analyze the effects of Pasternak foundation and ideal fluid on the natural frequencies and corresponding mode shapes of a rectangular plate. Hosseini-Hashemi et al. [35] have reported the natural frequencies of rectangular Mindlin plates coupled with stationary fluid. Furthermore, Eshaghi [36] has carried out the effect of magnetorheological fluid and aerodynamic damping for sandwich plates. By utilizing Galerkin method and Rayleigh-Ritz method, Zhou and Liu [37] have presented the analysis of hydroelastic vibrations of flexible rectangular tanks partially filled with liquid which accounted surface waves, bulging mode, and sloshing mode. An experimental investigation of free vibration of a floating composite sandwich plate with viscoelastic core has been provided by Rezvani and Kiasat [38]. Watts [39] has studied the vibrational characteristic of skew and trapezoidal plates with simply-supported and clamped boundary conditions in interaction with fluid by using a semi-analytical technique.

A classical method used in the last decades to obtain approximate solutions for the natural frequencies of beams, plates, and shells is the Rayleigh–Ritz method. Many different basic functions have been used in this method to guess the structural response in terms of the displacement parameters. For instance, Rahmani et al. [40] have used trigonometric functions for the free vibrational analysis of composite sandwich cylindrical shell. On the other hand, Chow et al. [41] have carried out the vibrational analysis of symmetrically laminated plates with the Rayleigh-Ritz method by utilizing admissible 2D orthogonal polynomials. An investigation has been done by using 2D orthogonal polynomials by Bhat [42] to analyze the flexural vibration of polygonal plates, whereas the Gram-Schmidt process has been used to generate the orthogonal two-variable polynomials. In order to use a two-variable function in the form of single series instead of two separate functions in the plate's in-plane directions, Liew [43] has presented the analysis of vibration of a rectangular plate. Comprehensive reviews on the Rayleigh-Ritz method and its application have been presented by Kumar[44], Pablo et al. [45] and Chakraverty et al. [46]. A study by Nallim [47] showed that it is beneficial to use the Rayleigh-Ritz method with orthogonal polynomials functions rather than other guess functions because of a much faster convergence rate. It is worth mentioning that the advantages of semi-analytical methods over numerical methods, such as the Finite Element Method (FEM), are their direct applicability to both linear and nonlinear equations without requiring linearization, discretization, or perturbation procedures [48]. Furthermore, the existence of solutions can be proved using semi-analytical methods.

Consequently, in this paper single series with two-variable orthogonal polynomials (orthogonal plate functions) will be used instead of double series to apply the Rayleigh-Ritz method.

To the best of the authors' knowledge, there is no research on the free vibration of sandwich plate with compressible core and different boundary conditions in contact with bounded fluid. The main novelty of the current study is to investigate the fluid-structure interaction effects on the vibrational characteristics of a rectangular sandwich plate in which the compressibility of the core and various boundary conditions are considered. The extended higher-order sandwich plate theory is used, in which both the in-plane and out-of-plane stresses in the core are considered. The distribution of the in-plane and transverse (out-of-plane) displacements of the core are assumed to cubic and quadratic, respectively. The effects of boundary conditions, aspect ratio, side-to-thickness ratio, thickness of the core to thickness of the face sheets ratio, face sheet to core flexural modulus ratio, and dimensions of the container on the natural frequencies of sandwich plate are studied in detail.

2. Mathematical Formulation

2.1. Sandwich Plate Formulation

We consider a rectangular sandwich plate with length a, width b, and total thickness h (Fig. 1). We assume that the sandwich plate is one of the vertical sides of a rigid tank with width c. The tank contains a fluid up to a depth d. We suppose that the fluid is inviscid, incompressible, and irrotational, and has mass density ρ_f. A Cartesian reference system *Oxyz* is fixed with the origin at a corner of the plate, the *x*- and *y*-axes along the in-plane directions of the plate, and the *z*-axis pointing towards the interior of the tank.

Fig. 2 illustrates the sandwich plate in detail. It is made up of three layers: a top face sheet with thicknessf_t, a core with thickness f_c, and a bottom face sheet with thickness f_b. Henceforth, indices t, b, and c denote quantities related to the top face sheet, bottom face sheet, and core, respectively.

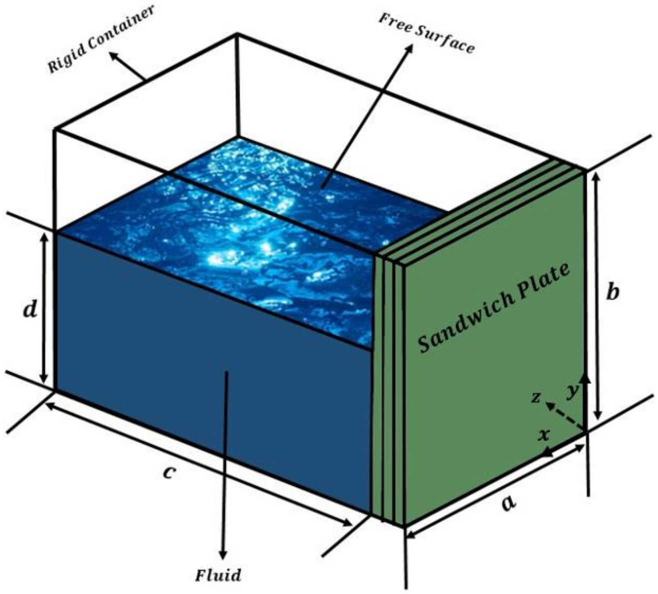

Fig. 1: A rectangular sandwich plate in contact with fluid

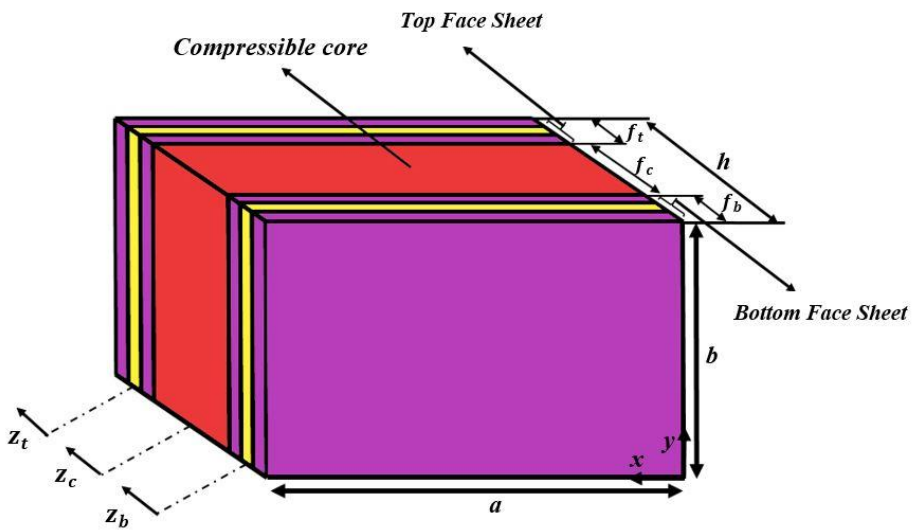

Fig. 2: Sandwich plate with length a, width b and total thickness h

By assuming small deformations and rotations in line with FSDT, the displacement fields for the top and bottom face sheets at time t are:

$$\begin{cases} u_i(x,y,z,t) = u_0^i(x,y,t) + z_i\psi_x^i(x,y,t) \\ v_i(x,y,z,t) = v_0^i(x,y,t) + z_i\psi_y^i(x,y,t)\,, \qquad (i=t,b) \\ \qquad w_i(x,y,t) = w_0^i(x,y,t) \end{cases} \tag{1}$$

in which u_0^i and v_0^i are the in-plane displacements in the $x-$ and $y-$ directions, respectively; w_0^i is the transverse displacement of the middle surface of the face sheets; ψ_x^i and ψ_y^i are the rotation component of the transverse normal about the $y-$ and $x-$ directions, respectively. For each

layer, a local transverse coordinate z_i is introduced pointing in the downward direction and measured from the local mid-plane.
The kinematic relations of the face sheets are as follows:

$$\begin{aligned}
&\varepsilon_{xx}^{i}(x,y,z_i,t)=u_{0,x}^{i}+z_i\psi_{x,x}^{i}=\varepsilon_{0xx}^{i}+z_i\kappa_x^{i}\\
&\varepsilon_{yy}^{i}(x,y,z_i,t)=v_{0,y}^{i}+z_i\psi_{y,y}^{i}=\varepsilon_{0yy}^{i}+z_i\kappa_y^{i}\\
&\gamma_{xy}^{i}(x,y,z_i,t)=u_{0,y}^{i}+v_{0,x}^{i}+z_i\left(\psi_{x,y}^{i}+\psi_{y,x}^{i}\right)=\gamma_{0xy}^{i}+z_i\kappa_{xy}^{i}\\
&\gamma_{xz}^{i}(x,y,z_i,t)=(\psi_x^{i}+w_{0,x}^{i})\\
&\gamma_{yz}^{i}(x,y,z_i,t)=\left(\psi_y^{i}+w_{0,y}^{i}\right)\qquad (i=t,b)
\end{aligned}\tag{2}$$

where:

$$\begin{aligned}
&\varepsilon_{0xx}^{i}=u_{0,x}^{i}\\
&\varepsilon_{0yy}^{i}=v_{0,y}^{i}\\
&\gamma_{0xy}^{i}=u_{0,y}^{i}+v_{0,x}^{i}\\
&\kappa_x^{i}=\psi_{x,x}^{i}\\
&\kappa_y^{i}=\psi_{y,y}^{i}\\
&\kappa_{xy}^{i}=\psi_{x,y}^{i}+\psi_{y,x}^{i}(i=t,b)
\end{aligned}\tag{3}$$

In present paper, cubic and quadratic polynomial distributions are assumed for the in-plane and transverse displacement fields of the core, respectively [49]:

$$\begin{aligned}
&u_c(x,y,z_c,t)=u_0(x,y,t)+z_cu_1(x,y,t)+z_c^2u_2(x,y,t)+z_c^3u_3(x,y,t)\\
&v_c(x,y,z_c,t)=v_0(x,y,t)+z_cv_1(x,y,t)+z_c^2v_2(x,y,t)+z_c^3v_3(x,y,t)\\
&w_c(x,y,z_c,t)=w_0(x,y,t)+z_cw_1(x,y,t)+z_c^2w_2(x,y,t)
\end{aligned}\tag{4}$$

u_i and $v_i(i=0,1,2,3)$ are the unknowns of the in-plane displacements of the core; $w_j(j=0,1,2)$ are the unknowns of the vertical displacements of the core.
The generalized strains for the core are as below:

$$\begin{aligned}
&\varepsilon_{xx}^{c}=u_{0,x}+z_cu_{1,x}+{z_c}^2u_{2,x}+{z_c}^3u_{3,x}\\
&\varepsilon_{yy}^{c}=v_{0,y}+z_cv_{1,y}+{z_c}^2v_{2,y}+{z_c}^3v_{3,y}\\
&\varepsilon_{zz}^{c}=w_1+2z_cw_2\\
&\gamma_{xy}^{c}=u_{0,y}+z_cu_{1,y}+{z_c}^2u_{2,y}+{z_c}^3u_{3,y}+v_{0,x}+z_cv_{1,x}+{z_c}^2v_{2,x}+{z_c}^3v_{3,x}\\
&\gamma_{xz}^{c}=u_1+2z_cu_2+3{z_c}^2u_3+w_{0,x}+z_cw_{1,x}+{z_c}^2w_{2,x}\\
&\gamma_{yz}^{c}=v_1+2z_cv_2+3{z_c}^2v_3+w_{0,y}+z_cw_{1,y}+{z_c}^2w_{2,y}
\end{aligned}\tag{5}$$

Similar to the kinematic relations for the face sheets, Eq. (3),we define:

$$\begin{aligned}
&\varepsilon_{0xx}^{c}=u_{0,x}\ ;\ \varepsilon_{1xx}^{c}=u_{1,x}\ ;\ \varepsilon_{2xx}^{c}=u_{2,x}\ ;\ \varepsilon_{3xx}^{c}=u_{3,x}\\
&\varepsilon_{0yy}^{c}=v_{0,x}\ ;\ \varepsilon_{1yy}^{c}=v_{1,x}\ ;\ \varepsilon_{2yy}^{c}=v_{2,x}\ ;\ \varepsilon_{3yy}^{c}=v_{3,x}\\
&\varepsilon_{0zz}^{c}=w_1\ ;\ \varepsilon_{1zz}^{c}=2w_2\ ;\ \gamma_{0xy}^{c}=u_{0,y}+v_{0,x}\ ;\ \gamma_{1xy}^{c}=u_{1,y}+v_{1,x}\\
&\gamma_{2xy}^{c}=u_{2,y}+v_{2,x}\ ;\ \gamma_{3xy}^{c}=u_{3,y}+v_{3,x}\ ;\ \gamma_{0xz}^{c}=u_1+w_{0,x}\\
&\gamma_{1xz}^{c}=2u_2+w_{1,x}\ ;\ \gamma_{2xz}^{c}=3u_3+w_{2,x}\ ;\ \gamma_{0yz}^{c}=v_1+w_{0,y}\\
&\gamma_{1yz}^{c}=2v_2+w_{1,y}\ ;\ \gamma_{2yz}^{c}=3v_3+w_{2,y}
\end{aligned}\tag{6}$$

The stress-strain relations for the top and bottom laminated composite face sheets are given by:

$$\begin{Bmatrix}\sigma_{xx}\\ \sigma_{yy}\\ \tau_{xy}\end{Bmatrix}=\begin{bmatrix}\bar{Q}_{11}&\bar{Q}_{12}&\bar{Q}_{16}\\ \bar{Q}_{12}&\bar{Q}_{22}&\bar{Q}_{26}\\ \bar{Q}_{16}&\bar{Q}_{26}&\bar{Q}_{66}\end{bmatrix}\begin{Bmatrix}\varepsilon_{xx}\\ \varepsilon_{yy}\\ \gamma_{xy}\end{Bmatrix},\qquad \begin{Bmatrix}\tau_{yz}\\ \tau_{xz}\end{Bmatrix}=\begin{bmatrix}\bar{Q}_{44}&\bar{Q}_{45}\\ \bar{Q}_{45}&\bar{Q}_{55}\end{bmatrix}\begin{Bmatrix}\gamma_{yz}\\ \gamma_{xz}\end{Bmatrix}\tag{7}$$

where $\bar{Q}_{ij}$ are the transformed stiffness constants for the layers. The stress resultants for the top and bottom laminated face sheets are obtained as follows:

$$\begin{Bmatrix} N_{xx}^{(i)} \\ N_{yy}^{(i)} \\ N_{xy}^{(i)} \end{Bmatrix} = \begin{bmatrix} A_{11}^{(i)} & A_{12}^{(i)} & A_{16}^{(i)} \\ A_{21}^{(i)} & A_{22}^{(i)} & A_{26}^{(i)} \\ A_{16}^{(i)} & A_{26}^{(i)} & A_{66}^{(i)} \end{bmatrix} \begin{Bmatrix} u_{0,x}^{i} \\ v_{0,y}^{i} \\ u_{0,x}^{i} + v_{0,y}^{i} \end{Bmatrix} + \begin{bmatrix} B_{11}^{(i)} & B_{12}^{(i)} & B_{16}^{(i)} \\ B_{21}^{(i)} & B_{22}^{(i)} & B_{26}^{(i)} \\ B_{16}^{(i)} & B_{26}^{(i)} & B_{66}^{(i)} \end{bmatrix} \begin{Bmatrix} \psi_{x,x}^{i} \\ \psi_{y,y}^{i} \\ \psi_{x,x}^{i} + \psi_{y,y}^{i} \end{Bmatrix} \quad (i = t, b) \tag{8}$$

$$\begin{Bmatrix} M_{xx}^{(i)} \\ M_{yy}^{(i)} \\ M_{xy}^{(i)} \end{Bmatrix} = \begin{bmatrix} B_{11}^{(i)} & B_{12}^{(i)} & B_{16}^{(i)} \\ B_{21}^{(i)} & B_{22}^{(i)} & B_{26}^{(i)} \\ B_{16}^{(i)} & B_{26}^{(i)} & B_{66}^{(i)} \end{bmatrix} \begin{Bmatrix} u_{0,x}^{i} \\ v_{0,y}^{i} \\ u_{0,x}^{i} + v_{0,y}^{i} \end{Bmatrix} + \begin{bmatrix} D_{11}^{(i)} & D_{12}^{(i)} & D_{16}^{(i)} \\ D_{21}^{(i)} & D_{22}^{(i)} & D_{26}^{(i)} \\ D_{16}^{(i)} & D_{26}^{(i)} & D_{66}^{(i)} \end{bmatrix} \begin{Bmatrix} \psi_{x,x}^{i} \\ \psi_{y,y}^{i} \\ \psi_{x,x}^{i} + \psi_{y,y}^{i} \end{Bmatrix} \quad (i = t, b) \tag{9}$$

$$\begin{Bmatrix} Q_{yz}^{(i)} \\ Q_{xz}^{(i)} \end{Bmatrix} = \begin{bmatrix} A_{44}^{(i)} & A_{45}^{(i)} \\ A_{45}^{(i)} & A_{55}^{(i)} \end{bmatrix} \begin{Bmatrix} w_{i,y} + \psi_{yi} \\ w_{i,x} + \psi_{xi} \end{Bmatrix} \quad (i = t, b) \tag{10}$$

where A_{ij},B_{ij} and $D_{ij} (i = 1,2, \dots ,6)$ are the elements of the extensional, extension-bending coupling, and bending stiffness matrices, respectively. Likewise, A_{ij} $(i, j = 4,5)$ are the elements of the transverse shear stiffness matrices. For the face sheets, these quantities are given by:

$$A_{ij} = \sum_{k=1}^{N} \left(\bar{Q}_{ij}\right)_k (z_k - z_{k-1}) \tag{11a}$$

$$B_{ij} = \frac{1}{2} \sum_{k=1}^{N} \left(\bar{Q}_{ij}\right)_k (z_k^2 - z_{k-1}^2) \tag{11b}$$

$$D_{ij} = \frac{1}{3} \sum_{k=1}^{N} \left(\bar{Q}_{ij}\right)_k (z_k^3 - z_{k-1}^3), \qquad (i, j) = 1,2,6 \tag{11c}$$

and:

$$A_{ij} = k_s \sum_{k=1}^{N} \left(\bar{Q}_{ij}\right)_k (z_k - z_{k-1}), \qquad (i, j) = 4,5 \tag{11d}$$

in which *N* is the total number of layers in the laminate, z_k and z_{k-1} are the distances of the top and bottom surfaces of the kth layer from the face sheet's mid-plane, respectively. Likewise, k_s is the shear correction factor which is taken to be $5/6$[18, 50].

According to equations (2-3) and (8-10), the strain energy of the top and bottom face sheets can be defined as follows:

$$U_i = \frac{1}{2}\int_0^a \int_0^b \left[N_{xx}^i \varepsilon_{0xx}^i + N_{yy}^i \varepsilon_{0yy}^i + N_{xy}^i \gamma_{0xy}^i + M_{xx}^i \kappa_x^i + M_{yy}^i \kappa_y^i + M_{xy}^i \kappa_{xy}^i + Q_{yz}^i \gamma_{yz}^i + Q_{xz}^i \gamma_{xz}^i\right] dy\, dx \tag{12}$$

$$(i = t, b)$$

On the other hand, by assuming that the core material is isotropic, the stress-strain relations are related to it as follows:

$$\begin{Bmatrix} \sigma_{xx}^c \\ \sigma_{yy}^c \\ \sigma_{zz}^c \\ \tau_{xz}^c \\ \tau_{yz}^c \\ \tau_{xy}^c \end{Bmatrix} = \begin{bmatrix} \frac{1}{E_1} & -\frac{\upsilon_{12}}{E_1} & -\frac{\upsilon_{13}}{E_1} & 0 & 0 & 0 \\ -\frac{\upsilon_{12}}{E_1} & \frac{1}{E_2} & -\frac{\upsilon_{23}}{E_2} & 0 & 0 & 0 \\ -\frac{\upsilon_{13}}{E_1} & -\frac{\upsilon_{23}}{E_2} & \frac{1}{E_3} & 0 & 0 & 0 \\ 0 & 0 & 0 & \frac{1}{G_{23}} & 0 & 0 \\ 0 & 0 & 0 & 0 & \frac{1}{G_{31}} & 0 \\ 0 & 0 & 0 & 0 & 0 & \frac{1}{G_{12}} \end{bmatrix}^{-1} \begin{Bmatrix} \varepsilon_{xx}^c \\ \varepsilon_{yy}^c \\ \varepsilon_{zz}^c \\ \gamma_{xz}^c \\ \gamma_{yz}^c \\ \gamma_{xy}^c \end{Bmatrix} \tag{13}$$

in whichE_i and G_{ij} are the Young and shear modulus.

The stress resultants of the core are given by:

$$\begin{aligned}
\{N_{xx}^c, M_{nxx}^c\} &= \int_{-\frac{f_c}{2}}^{\frac{f_c}{2}} (1, z_c^n)\sigma_{xx}^c dz_c \\
\{N_{yy}^c, M_{nyy}^c\} &= \int_{-\frac{f_c}{2}}^{\frac{f_c}{2}} (1, z_c^n)\sigma_{yy}^c dz_c \\
\{N_{xy}^c, M_{nxy}^c\} &= \int_{-\frac{f_c}{2}}^{\frac{f_c}{2}} (1, z_c^n)\tau_{xy}^c dz_c \\
\{Q_{xz}^c, M_{Qnxz}^c\} &= \int_{-\frac{f_c}{2}}^{\frac{f_c}{2}} (1, z_c^n)\tau_{xz}^c dz_c \\
\{Q_{yz}^c, M_{Qnyz}^c\} &= \int_{-\frac{f_c}{2}}^{\frac{f_c}{2}} (1, z_c^n)\tau_{yz}^c dz_c \\
\{R_z^c, M_z^c\} &= \int_{-\frac{f_c}{2}}^{\frac{f_c}{2}} (1, z_c^n)\sigma_{zz}^c dz_c
\end{aligned} \tag{14}$$

According to equations (5-6) and (14), the strain energy of the core can be defined as follows:

$$
\begin{aligned}
U_c = \frac{1}{2}\int_0^a \int_0^b \big[& N_{xx}^c \varepsilon_{0xx}^c + M_{1xx}^c \varepsilon_{1xx}^c + M_{2xx}^c \varepsilon_{2xx}^c + M_{3xx}^c \varepsilon_{3xx}^c + N_{yy}^c \varepsilon_{0yy}^c \\
& + M_{1yy}^c \varepsilon_{1yy}^c + M_{2yy}^c \varepsilon_{2yy}^c + M_{3yy}^c \varepsilon_{3yy}^c + R_z^c \varepsilon_{0zz}^c + M_z^c \varepsilon_{1zz}^c \\
& + N_{xy}^c \gamma_{0xy}^c + M_{1xy}^c \gamma_{1xy}^c + M_{2xy}^c \gamma_{2xy}^c + M_{3xy}^c \gamma_{3xy}^c + Q_{xz}^c \gamma_{0xz}^c \\
& + M_{Q1xz}^c \gamma_{1xz}^c + M_{Q2xz}^c \gamma_{2xz}^c + Q_{yz}^c \gamma_{0yz}^c + M_{Q1yz}^c \gamma_{1yz}^c \\
& + M_{Q2yz}^c \gamma_{2yz}^c \big] dy\, dx
\end{aligned} \tag{15}
$$

Also, the kinetic energy of the top and bottom face sheets and the core are obtained as follows:

$$
\begin{aligned}
T_i = \frac{1}{2}\int_0^a \int_0^b \Big[& I_0^i \big((\dot{u}_0^i)^2 + (\dot{v}_0^i)^2 + (\dot{w}_0^i)^2 \big) + 2 I_1^i \big(\dot{u}_0^i \dot{\psi}_x^i + \dot{v}_0^i \dot{\psi}_y^i \big) \\
& + I_2^i \left(\left(\dot{\psi}_x^i \right)^2 + \left(\dot{\psi}_y^i \right)^2 \right) \Big] dy\, dx, \qquad (i = t, b)
\end{aligned} \tag{16}
$$

$$
\begin{aligned}
T_c = \frac{1}{2}\int_0^a \int_0^b [& I_0^c ({w_0}^2 + {u_0}^2 + {v_0}^2) + 2 I_1^c (w_0 w_1 + v_0 v_1 + u_0 u_1) \\
& + I_2^c ({w_1}^2 + 2 w_0 w_2 + {v_1}^2 + 2 v_0 v_2 + {u_1}^2 + 2 u_0 u_2) \\
& + 2 I_3^c (w_1 w_2 + v_1 v_2 + v_0 v_3 + u_1 u_2 + u_0 u_3) \\
& + I_4^c ({w_2}^2 + {v_2}^2 + 2 v_1 v_3 + {u_2}^2 + 2 u_1 u_3) + 2 I_5^c (v_2 v_3 + u_2 u_3) \\
& + I_6^c ({u_3}^2 + {v_3}^2)] dy\, dx
\end{aligned} \tag{17}
$$

where $I_j^i (j = 0,1,2; i = t, b)$ are the inertia terms of the face sheets and $I_j^c (j = 0,1, \dots ,6)$ are the inertia terms of the core, respectively defined as follows:

$$
\begin{aligned}
& \left(I_0^i, I_1^i, I_2^i \right) = \int_{-f_i/2}^{f_i/2} \rho^i (1, z_i, z_i^2) dz_i \; (i = t, b) \\
& (I_0^c, I_1^c, I_2^c, I_3^c, I_4^c, I_5^c, I_6^c) = \int_{-f_c/2}^{f_c/2} \rho^c (1, z_c, z_c^2, z_c^3, z_c^4, z_c^5, z_c^6) dz_c
\end{aligned} \tag{18}
$$

2.2. Compatibility Conditions

Since there is no slip between the core and face sheets, the compatibility conditions at the top and the bottom face–core interface are given as follows:

$$
\begin{aligned}
& u_c \left(z_c = -\frac{f_c}{2} \right) = u_0^b + \frac{1}{2} f_b \psi_x^b \\
& v_c \left(z_c = -\frac{f_c}{2} \right) = v_0^b + \frac{1}{2} f_b \psi_y^b \\
& w_c \left(z_c = -\frac{f_c}{2} \right) = w_0^b \\
& u_c \left(z_c = \frac{f_c}{2} \right) = u_0^t - \frac{1}{2} f_t \psi_x^t \\
& v_c \left(z_c = \frac{f_c}{2} \right) = v_0^t - \frac{1}{2} f_t \psi_y^t \\
& w_c \left(z_c = \frac{f_c}{2} \right) = w_0^t
\end{aligned} \tag{19}
$$

By substituting equations (1) and (4) into the above equation, the compatibility conditions are obtained:

$$
u_0 - u_1 \frac{f_c}{2} + u_2 \frac{f_c^2}{4} - u_3 \frac{f_c^3}{8} = u_0^b + \psi_x^b \frac{f_b}{2}
$$

$$v_0 - v_1\frac{f_c}{2} + v_2\frac{f_c^2}{4} - v_3\frac{f_c^3}{8} = v_0^b + \psi_y^b\frac{f_b}{2}$$
$$w_0 - w_1\frac{f_c}{2} + w_2\frac{f_c^2}{4} = w_0^b \quad (20)$$
$$u_0 + u_1\frac{f_c}{2} + u_2\frac{f_c^2}{4} + u_3\frac{f_c^3}{8} = u_0^t - \psi_x^t\frac{f_t}{2}$$
$$v_0 + v_1\frac{f_c}{2} + v_2\frac{f_c^2}{4} + v_3\frac{f_c^3}{8} = v_0^t - \psi_y^t\frac{f_t}{2}$$
$$w_0 + w_1\frac{f_c}{2} + w_2\frac{f_c^2}{4} = w_0^t$$

For ease of calculation, the relations between the dependent coefficients are calculated and the number of unknowns of the problem is reduced. The relations between displacement dependent parameters in the core are derived as the following:

$$u_2 = (2(u_0^b + u_0^t) + f_b\psi_x^b - f_t\psi_x^t - 4u_0)/f_c^2$$
$$u_3 = (4(u_0^t - u_0^b) - 2(f_b\psi_x^b + f_t\psi_x^t) - 4f_c u_1)/f_c^3$$
$$v_2 = (2(v_0^b + v_0^t) + f_b\psi_y^b - f_t\psi_y^t - 4v_0)/f_c^2 \quad (21)$$
$$v_3 = (4(v_0^t - v_0^b) - 2(f_b\psi_y^b + f_t\psi_y^t) - 4f_c v_1)/f_c^3$$
$$w_2 = 2(w_0^t + w_0^b - 2w_0)/f_c^2$$
$$w_1 = (w_0^t - w_0^b)/f_c$$

2.3. Fluid Formulations

There are two well-known vibrational modes of the fluid-structure systems: the bulging and sloshing modes. Vibrations of flexible structure that stimulate fluid are related to the bulging modes. Conversely, sloshing modes are caused by the rigid body movement of the container that oscillates in the fluid free-surface [51]. The fluid is assumed to be inviscid, incompressible, and irrotational. Now, by using the principle of superposition, the fluid velocity potential will be written as follow:

$$\Phi_O = \Phi_B + \Phi_S \quad (22)$$

where Φ_B and Φ_S are the fluid velocity potential associated with bulging and sloshing modes, respectively. On the other hand the fluid velocity potential can be divided into two separate segments: Spatial velocity potential and a harmonic time function [51]:

$$\Phi_O(x,y,z,t) = \varphi_O(x,y,z)\dot{T}(t) = i\bar{\omega}\varphi_O(x,y,z)e^{i\bar{\omega}t} \quad (23)$$

in which $\bar{\omega}$ is the natural frequency and $i = \sqrt{-1}$ is the imaginary unit.

To satisfy the three-dimensional Laplace equation, the fluid velocity potential is introduced:

$$\nabla^2\varphi_O = \nabla^2\varphi_B + \nabla^2\varphi_S = 0 \rightarrow \nabla^2\varphi_B = 0\,, \nabla^2\varphi_S = 0 \quad (24)$$

where ∇^2 is the Laplace operator.

The boundary conditions of the rigid walls of the container can be given as:

$$\left.\frac{\partial\varphi_B}{\partial x}\right|_{x=0,a} = 0, \qquad \left.\frac{\partial\varphi_B}{\partial y}\right|_{y=0} = 0, \qquad \left.\frac{\partial\varphi_B}{\partial z}\right|_{z=c} = 0 \quad (25a)$$

$$\left.\frac{\partial\varphi_S}{\partial x}\right|_{x=0,a} = 0, \qquad \left.\frac{\partial\varphi_S}{\partial y}\right|_{y=0} = 0, \qquad \left.\frac{\partial\varphi_S}{\partial z}\right|_{z=0,c} = 0 \quad (25b)$$

By neglecting the effect of free surface waves, φ_B must satisfy the following boundary conditions:

$$\varphi_B|_{y=d} = 0 \tag{26}$$

Also at the fluid-contacting surface, the velocity components of the fluid and top face sheet of the sandwich plate in the transverse direction must be equal:

$$\left.\frac{\partial \Phi_B}{\partial z}\right|_{z=0} = \frac{\partial w_t(x,y,t)}{\partial t} \tag{27}$$

where $w_t(x,y,t)$ is the transverse deflection of the top face sheet in sandwich plate. The linearized sloshing condition at the fluid free surface can be written as:

$$\left.\frac{\partial \Phi_O}{\partial y}\right|_{y=d} = \frac{\overline{\omega}^2}{g}\Phi_O|_{y=d} \tag{28}$$

where g is the gravity acceleration. By substituting Eq. (22) into (28), and recalling Eq. (26), one obtains:

$$\left.\frac{\partial \Phi_B}{\partial y}\right|_{y=d} + \left.\frac{\partial \Phi_S}{\partial y}\right|_{y=d} = \frac{\overline{\omega}^2}{g}\Phi_S|_{y=d} \tag{29}$$

Multiplying the above equation by $\rho_f \Phi_S$ and then integrating over the fluid free surface, we have:

$$U_{\varphi_B} + U_{\varphi_S} = \overline{\omega}^2 T_{\varphi_S} \tag{30}$$

in which:

$$\begin{aligned}
U_{\varphi_B} &= \rho_f \int_0^a \int_0^c \Phi_S \left.\frac{\partial \Phi_B}{\partial y}\right|_{y=d} dzdx \\
U_{\varphi_S} &= \rho_f \int_0^a \int_0^c \Phi_S \left.\frac{\partial \Phi_S}{\partial y}\right|_{y=d} dzdx \\
T_{\varphi_S} &= \frac{\rho_f}{g} \int_0^a \int_0^c {\Phi_S}^2|_{y=d}\, dzdx
\end{aligned} \tag{31}$$

By performing the method of separation of variables and using the boundary conditions Eq. (25), the fluid velocity potentials can be obtained by solving Eq. (24):

$$\Phi_B(x,y,z,t) = i\,\overline{\omega}\varphi_B(x,y,z)e^{i\overline{\omega}t} \tag{32a}$$

$$\varphi_B(x,y,z) = \varphi_{Bx}(x)\varphi_{By}(y)\varphi_{Bz}(z) \tag{32b}$$

$$\frac{\partial^2 \varphi_B}{\partial x^2} + \frac{\partial^2 \varphi_B}{\partial y^2} + \frac{\partial^2 \varphi_B}{\partial z^2} = 0 \tag{32c}$$

By substituting Eq. (32b) into (32c), we get:

$$\frac{1}{\varphi_{Bx}(x)}\frac{d^2\varphi_{Bx}(x)}{dx^2} + \frac{1}{\varphi_{By}(y)}\frac{d^2\varphi_{By}(y)}{dy^2} + \frac{1}{\varphi_{Bz}(z)}\frac{d^2\varphi_{Bz}(z)}{dz^2} = 0 \tag{33}$$

Eq. (33) can be separated as:

$$\frac{1}{\varphi_{Bx}(x)}\frac{d^2\varphi_{Bx}(x)}{dx^2} = -p_1^2 \tag{34a}$$

$$\frac{1}{\varphi_{By}(y)}\frac{d^2\varphi_{By}(y)}{dy^2} = -q_1^2 \tag{34b}$$

$$\frac{1}{\varphi_{Bz}(z)}\frac{d^2\varphi_{Bz}(z)}{dz^2} = (p_1^2 + q_1^2) \tag{34c}$$

where $-p_1^2$ and $-q_1^2$ are optional nonnegative real number. The general solution of the above equations ((34a),(34b) and (34c)) are:

$$\varphi_{Bx}(x) = a_1\sin(p_1 x) + a_2\cos(p_1 x) \tag{35a}$$

$$\varphi_{By}(y) = a_3\, sin(q_1 y) + a_4 cos(q_1 y) \tag{35b}$$

$$\varphi_{Bz}(z) = a_5 e^{\sqrt{p_1^2+q_1^2}z} + a_6 e^{-\sqrt{p_1^2+q_1^2}z} \tag{35a}$$

By applying the boundary conditions Eq. (25) and inserting into Eq. (32a), the expression of the fluid velocity potential for the bulging modes are as follows:

$$\Phi_B(x,y,z,t) = \sum_{l=0}^{\infty}\sum_{k=0}^{\infty} i\varpi\Lambda_{lk}(t)\cos(\frac{l\pi x}{a})\cos(\frac{(2k+1)\pi y}{2d})\{e^{\sigma z} + e^{\sigma(2c-z)}\} \tag{36}$$

For $l,k = 0,1,2,\dots,\ \ 0 \le x \le a, \quad 0 \le y \le b, \quad 0 \le z \le c$

where:

$$\sigma = \pi\sqrt{\left(\frac{l}{a}\right)^2 + \left(\frac{2k+1}{2d}\right)^2} \tag{37}$$

The compatibility condition at the fluid-sandwich plate interface is:

$$\sum_{l=0}^{\infty}\sum_{k=0}^{\infty} i\varpi\Lambda_{lk}(t)\sigma(1-e^{2c\sigma})cos\left(\frac{l\pi x}{a}\right)cos\left(\frac{(2k+1)\pi y}{2d}\right) = \frac{\partial w_t(x,y,t)}{\partial t} \tag{38}$$

The above equation can be considered as a double Fourier series, whose coefficient $\Lambda_{lk}(t)$are determined as follows:

$$\Lambda_{lk}(t) = \frac{coeff}{i\varpi ad\sigma(1-e^{2c\sigma})}\int_0^a\int_0^d \frac{\partial w_t(x,y,t)}{\partial t}\ cos\left(\frac{l\pi x}{a}\right)cos\left(\frac{(2k+1)\pi y}{2d}\right)dydx \tag{39}$$

in which:

$$coeff = \begin{cases} 1, & if\ l\ and\ k = 0 \\ 2, & if\ l\ or\ k = 0 \\ 4, & if\ l\ and\ k \neq 0 \end{cases} \tag{40}$$

In a similar way, to calculate the fluid velocity potential associated with sloshing mode, by using the separation variable method and with the help of boundary conditions Eq. (25b), the general solution is:

$$\Phi_S(x,y,z,t) = \sum_{i=0}^{\infty}\sum_{j=0}^{\infty} i\varpi\Gamma_{ij}(t)cos\left(\frac{i\pi x}{a}\right)\cosh(\tau y)cos\left(\frac{j\pi z}{c}\right) \tag{41}$$

where $\Gamma_{ij}(t)$are the undetermined coefficients and:

$$\tau = \pi\sqrt{\left(\frac{i}{a}\right)^2 + \left(\frac{j}{c}\right)^2} \tag{42}$$

Since the fluid is considered to be incompressible, inviscid and irrotational, the kinetic energy of the fluid is as follows:

$$T_f = \frac{1}{2}\rho_f \int_V |\nabla\Phi_O|^2 dV \tag{43}$$

where ρ_f, V and $\nabla\Phi_O$ are the fluid density, fluid domain and velocity vector, respectively. In order to achieve total kinetic energy of the fluid in addition to considering boundary conditions Eq. (25) and compatibility conditions Eq. (27), the divergence theorem need to be adapted to Eq. (43).

$$T_f = T_{fB} + T_{fS} = -\frac{1}{2}\rho_f \int_0^a \int_0^d \left(\Phi_O \frac{\partial \Phi_O}{\partial z}\right)\Big|_{z=0} dA$$
$$= -\frac{1}{2}\rho_f \int_0^a \int_0^d (\Phi_B + \Phi_S)|_{z=0} \left(\frac{\partial w_t}{\partial t}\right) dydx \quad (44)$$

3. Governing Equations and Corresponding Boundary Conditions

The Hamiltonian principle for the free vibration analysis of a wet sandwich panel is stated as follows.

$$\delta \int_{t_i}^{t_f} (T_p + T_f - U_p) dt = 0 \quad (45)$$

In the above equation, T_p and U_p are the kinetic and potential (strain) energies of the sandwich plate, respectively; T_f is the kinetic energy of the fluid presented in Eq. (44). By inserting these energy expressions into Hamilton's principle, the governing equations of motion and corresponding boundary conditions are obtained as presented in Appendix A.

3.1. Solution Method

Displacement components of the face sheets and the core can be expressed by utilizing two-variable orthogonal polynomials by single series as follows:

$$\begin{aligned}
&u^t(x,y) = \sum_{i=1}^{m} u_i^t \lambda_i^{u^t}(x,y) && v^t(x,y) = \sum_{i=1}^{m} v_i^t \lambda_i^{v^t}(x,y)\\
&w^t(x,y) = \sum_{i=1}^{m} w_i^t \lambda_i^{w^t}(x,y) && \psi_x^t(x,y) = \sum_{i=1}^{m} \psi_{x_i}^t \lambda_i^{x^t}(x,y)\\
&\psi_y^t(x,y) = \sum_{i=1}^{m} \psi_{y_i}^t \lambda_i^{y^t}(x,y) && u^b(x,y) = \sum_{i=1}^{m} u_i^b \lambda_i^{u^b}(x,y)\\
&v^b(x,y) = \sum_{i=1}^{m} v_i^b \lambda_i^{v^b}(x,y) && w^b(x,y) = \sum_{i=1}^{m} w_i^b \lambda_i^{w^b}(x,y)\\
&\psi_x^b(x,y) = \sum_{i=1}^{m} \psi_{x_i}^b \lambda_i^{x^b}(x,y) && \psi_y^b(x,y) = \sum_{i=1}^{m} \psi_{y_i}^b \lambda_i^{y^b}(x,y)\\
&u_0(x,y) = \sum_{i=1}^{m} u_{0_i} \lambda_i^{u^c}(x,y) && u_1\ (x,y) = \sum_{i=1}^{m} u_{1_i} \lambda_i^{{u_1}^c}(x,y)\\
&v_0(x,y) = \sum_{i=1}^{m} v_{0_i} \lambda_i^{v^c}(x,y) && v_1\ (x,y) = \sum_{i=1}^{m} v_{1_i} \lambda_i^{{v_1}^c}(x,y)\\
&w_0(x,y) = \sum_{i=1}^{m} w_{0_i} \lambda_i^{w^c}(x,y)
\end{aligned} \quad (46)$$

in which (w_i^t, v_i^t, u_i^t, $\psi_{x_i}^t$, $\psi_{y_i}^t$, w_i^b,v_i^b, u_i^b, $\psi_{x_i}^b$, $\psi_{y_i}^b$, w_{0_i}, v_{0_i}, u_{0_i}, v_{1_i}, u_{1_i}) are unknown coefficients and $\lambda_i^k(k = w^t, w^b, w^c, \dots, {u_1}^c)$ are shape functions that must be chosen to satisfy the essential boundary conditions. As mentioned earlier, various shape functions including polynomial and trigonometric functions, have been used to satisfy the essential boundary conditions. Bhat [42] and Liew [43] provided the Gram-Schmidt process to generate two-variable orthogonal polynomials functions. The members of the orthogonal polynomials are generated as follows (see Appendix B):

$$\lambda_i^k(x,y) = \left(f_i(x,y) - a_{i,1}\right)\lambda_1^k(x,y) - a_{i,2}\lambda_2^k(x,y) - a_{i,3}\lambda_3^k(x,y) - \cdots \\ - a_{i,i-1}\lambda_{i-1}^k(x,y) \tag{47}$$

where $f_i(x,y)$ is the weight function that is represented by $(1, x, y, x^2, xy, y^2, \dots, x^{i-n}y^n)$ where $(i = 1, \dots, m \; and \; n = 0, \dots, m)$ and $a_{i,i-1}$ is calculated as follows [42, 43]:

$$a_{i.i-1} = \frac{\int_0^a \int_0^b f_i \lambda_1^k(x,y)\lambda_{i-1}^k(x,y)\, dydx}{\int_0^a \int_0^b \lambda_{i-1}^k(x,y)\lambda_{i-1}^k(x,y)\, dydx} \tag{48}$$

The orthogonality relationship must be satisfied by the generated set of plate functions:

$$\int_0^a \int_0^b \lambda_i^k(x,y)\, \lambda_j^k(x,y) dxdy = \begin{cases} 0 \;\; if \;\; i \neq j \\ \\ \epsilon_{ij} \neq 0 \;\; if \;\; i = j \end{cases} \tag{49}$$

where ϵ_{ij} is a non-zero value. Using the above method, the displacement components can be considered as single series [42].

3.2. Rayleigh-Ritz Method

The Lagrangian function of the fluid-sandwich plate coupled system expresses:

$$\Pi = \sum (Strain\ Energy)_{max} - \sum (Kinetic\ Energy)_{max} \tag{50}$$

To minimize the above equation with respect to the unknown coefficients, we impose:

$$\frac{\partial \Pi}{\partial q} = 0 \tag{51}$$

in which q is the vector of generalized coordinates including unknown coefficients of the admissible trial functions which have been demonstrated in Eq. (41) and Eq. (46) (i.e. q=$\left\{w_i^t, v_i^t, u_i^t, \psi_{x_i}^t, \psi_{y_i}^t, w_i^b, v_i^b, u_i^b, \psi_{x_i}^b, \psi_{y_i}^b, w_{0_i}, v_{0_i}, u_{0_i}, v_{1_i}, u_{1_i}, \Gamma_{ij}\right\}^T$). The eigenvalue problem is obtained by employing Eq. (51):

$$\left(K_p\right)\mathrm{H}_i - \overline{\omega}^2\left[\left(M_p + M_{fB}\right)\mathrm{H}_i + M_{fS}\Gamma_{m,n}\right] = 0 \tag{52}$$

where $\mathrm{H}_i = \left\{w_i^t, v_i^t, u_i^t, \psi_{x_i}^t, \psi_{y_i}^t, w_i^b, v_i^b, u_i^b, \psi_{x_i}^b, \psi_{y_i}^b, w_{0_i}, v_{0_i}, u_{0_i}, v_{1_i}, u_{1_i}, \Gamma_{ij}\right\}^T$ and:

$$K_p = \frac{\partial^2 U_p}{\partial q_i \partial q_j}\ , \qquad M_p = \frac{1}{\overline{\omega}^2}\frac{\partial^2 T_p}{\partial q_i \partial q_j}\ , \\ M_{fB} = \frac{1}{\overline{\omega}^2}\frac{\partial^2 T_{fB}}{\partial q_i \partial q_j}\ , \qquad M_{fS} = \frac{1}{\overline{\omega}^2}\frac{\partial^2 T_{fS}}{\partial q_i \partial q_j}\ , \tag{53}$$

Eq. (52) cannot be solved without having an expression for $\Gamma_{m,n}$.Thus Eq. (30) has to be added to Eq. (53):

$$\begin{bmatrix} K_p & 0 \\ K_{\varphi_B} & K_{\varphi_S} \end{bmatrix} \begin{Bmatrix} H_i \\ \Gamma_{m,n} \end{Bmatrix} - \overline{\omega}^2 \begin{bmatrix} M_p + M_{fB} & M_{fS} \\ 0 & M_{\varphi_S} \end{bmatrix} \begin{Bmatrix} H_i \\ \Gamma_{m,n} \end{Bmatrix} = 0 \tag{54}$$

in which:

$$K_{\varphi_B} = \frac{\partial^2 U_{\varphi_B}}{\partial q_i \partial q_j} = \frac{\partial^2 U_{\varphi_B}}{\partial H_i \partial \Gamma_{m,n}} \tag{55a}$$

$$K_{\varphi_S} = \frac{\partial^2 U_{\varphi_S}}{\partial q_i \partial q_j} = \frac{\partial^2 U_{\varphi_S}}{\partial \Gamma_{i,j} \partial \Gamma_{m,n}} \tag{55b}$$

$$M_{\varphi_S} = \frac{\partial^2 T_{\varphi_S}}{\partial q_i \partial q_j} = \frac{\partial^2 T_{\varphi_S}}{\partial \Gamma_{i,j} \partial \Gamma_{m,n}} \tag{55c}$$

Equation (54) is a standard eigenvalue problem which the natural frequencies (eigenvalue) and the mode shapes (eigenvector) of the sandwich plate in contact with fluid can be determined.

4. Numerical Results and Discussion

In the following, a convergence study of the proposed method is conducted at first. Then, in order to validate the results of this paper, comparison study has been done with published papers in literature. Eventually, the wet natural frequencies of sandwich plate with different boundary conditions in contact with fluid are demonstrated and the effects of side-to-thickness ratio, thickness of the core to thickness of the face sheets ratio, flexural modulus of the face sheet to that of the core ratio, dimensions of the tank and aspect ratios on the natural frequencies are discussed in details. All calculations have been carried out by applying the commercial software, Matlab (version 2018a) and the outcomes are displayed in graphical and tabular styles.

The material properties for the core and face sheets used in the following examples are given in Table 1.

Table 1: The material properties for various types of sandwich plates

		Material No.					
Property	Unit	M_1[22]	M_2[22]	M_3[52]	M_4[52]	M_5[52]	M_6[52]
E_1	GPa	0.10363	24.51	0.00689	131	0.5776	276
E_2	GPa	0.10363	7.77	0.00689	10.34	0.5776	6.9
E_3	GPa	0.10363	7.77	0.00689	10.34	0.5776	6.9
G_{12}	GPa	0.05	3.34	0.00345	6.895	0.1079	6.9
G_{23}	GPa	0.05	1.34	0.00345	6.895	0.2221	6.9
G_{13}	GPa	0.05	3.34	0.00345	6.205	0.1079	6.9
v_{12}		0.33	0.078	0	0.22	0.0025	0.25
v_{23}		0.33	0.49	0	0.22	0.0025	0.25
v_{13}		0.33	0.078	0	0.49	0.0025	0.3
ρ	kg/m^3	130	1800	97	1627	1000	681.8

4.1. Convergence Study

In this section, the convergence of the response has inspected with respect to the number of the terms of series. Table 2 shows the first four dimensionless dry natural frequencies of sandwich plate with various boundary conditions and lay-up [0/90/0/Core/0/90/0] for a different number of terms of series. The dimensionless natural frequency (ω) has been calculated based on $\omega = \varpi a^2 \sqrt{\rho_c / E_c}\,/h$. Also, ρ_c and E_c are the density and modulus of the core, respectively and h is the total thickness of the sandwich plate. The geometrical parameters have been already depicted in Figs. 1 and 2.

Table 2: Convergence study of first four dimensionless dry natural frequencies parameters ($\omega = \overline{\omega} a^2 \sqrt{\rho_c / E_c} / h$) of a sandwich plate ($a/b = 1, a/h = 10$ and $h_c/h = 0.88$)

M	Boundary conditions							
	SSSS				CCCC			
	ω_1	ω_2	ω_3	ω_4	ω_1	ω_2	ω_3	ω_4
10	14.2844	27.6400	28.1594	36.4457	18.4162	31.7830	32.1142	44.8576
15	14.2843	26.2126	26.8479	36.2009	18.2196	28.8885	29.3947	42.9198
20	14.2827	26.2122	26.8455	34.5758	18.1153	28.7599	29.1353	37.0841
25	14.2820	26.2086	26.8224	34.5695	18.0103	28.5495	29.0170	36.8868
30	14.2820	26.1842	26.8222	34.5591	17.9639	28.4133	28.9504	36.7771
35	14.2820	26.1842	26.8222	34.5165	17.9478	28.3883	28.8626	36.7106
40	14.2820	26.1842	26.8222	34.5165	17.9478	28.3883	28.8626	36.7106
	SSSF				CCCF			
10	10.5006	18.7186	26.2797	32.1588	13.9496	22.1572	27.4178	36.0943
15	10.4921	18.3579	24.8871	30.8953	13.8230	20.6926	26.8285	34.0270
20	10.4891	18.3357	24.8684	29.8088	13.7221	20.5091	26.6335	31.8340
25	10.4889	18.3234	24.8442	29.7261	13.6645	20.3409	26.4929	31.6590
30	10.4886	18.3217	24.8435	29.7074	13.6600	20.2791	26.4849	31.5179
35	10.4886	18.3217	24.8432	29.6955	13.6366	20.2508	26.3918	31.4783
40	10.4886	18.3217	24.8432	29.6955	13.6366	20.2508	26.3918	31.4783
	SSCF				CSCS			
10	10.9920	20.3254	26.6838	34.4669	16.3961	29.6513	30.5919	40.7456
15	10.9521	19.3627	25.1142	32.9630	16.3169	27.8809	27.9451	40.2995
20	10.9458	19.2957	25.0303	30.5796	16.2876	27.7276	27.9400	36.0144
25	10.9381	19.1950	24.9896	30.4578	16.2065	27.6518	27.7853	35.9232
30	10.9319	19.1317	24.9799	30.2939	16.1656	27.5669	27.6220	35.8057
35	10.9319	19.1317	24.9796	30.2877	16.1656	27.5669	27.6220	35.8010
40	10.9319	19.1317	24.9796	30.2877	16.1656	27.5669	27.6220	35.8010

Another convergence study has been done on the dimensionless wet natural frequencies of sandwich plate with different boundary conditions and lay-up [0/90/0/Core/0/90/0] coupled with fluid. As shown in tables 2 and 3, as the number of terms of series increases, the natural frequencies converge to the specified amounts. Thus, for the upcoming results, we use $M = 40$ for the number of terms of series for the plate deformation components and $M_1 = N_1 = 8$ for the fluid velocity potential.

Table 3: Convergence study of first four dimensionless wet natural frequencies parameters ($\omega = \overline{\omega} a^2 \sqrt{\rho_c / E_c} / h$) of a sandwich plate coupled with fluid ($a/b = 2, a/h = 10$, $h_c/h = 0.88$ and $d/b = 0.2$)

M	$M_1 \times N_1$	Boundary conditions	
		SSSS	CCCC

		ω_1	ω_2	ω_3	ω_4	ω_1	ω_2	ω_3	ω_4
15	2×2	25.9477	34.2948	47.2739	48.0081	30.1746	38.1394	53.1808	54.4372
20	3×3	25.9465	34.1848	44.9212	48.0014	30.0706	37.6279	48.1636	52.9328
25	4×4	25.9419	34.1673	44.7515	47.8810	29.9351	37.4770	47.9115	52.3483
30	5×5	25.9413	34.1563	44.6050	47.7841	29.7478	37.2828	47.6878	51.9772
35	6×6	25.9410	34.1543	44.5600	47.7779	29.7365	37.1099	47.4213	51.8755
40	7×7	25.9395	34.1533	44.5589	47.6196	29.7011	37.0832	47.3163	51.6214
40	8×8	25.9395	34.1533	44.5589	47.6196	29.7011	37.0832	47.3163	51.6214
		SSSF				CCCF			
15	2×2	12.3850	26.4292	35.4486	42.6183	17.2727	29.0542	37.7840	42.7930
20	3×3	12.3822	26.3780	35.4355	39.9279	17.1772	28.7743	37.4871	41.9909
25	4×4	12.3818	26.3551	35.3913	39.8289	17.1025	28.6350	37.1648	41.7263
30	5×5	12.3817	26.3515	35.3819	39.7188	17.0584	28.5166	36.9306	41.5948
35	6×6	12.3817	26.3498	35.3808	39.7042	17.0538	28.4820	36.8567	41.5531
40	7×7	12.3816	26.3495	35.3697	39.7000	17.0261	28.4505	36.7397	41.4528
40	8×8	12.3816	26.3495	35.3697	39.7000	17.0261	28.4505	36.7397	41.4528
		SSCF				CSCS			
15	2×2	15.3044	27.4546	37.1240	43.6059	29.2714	36.8525	51.8344	52.6429
20	3×3	15.2990	27.2976	37.0650	40.6043	29.2458	36.5410	47.1749	52.6288
25	4×4	15.2605	27.2595	36.7582	40.3717	29.1080	36.4552	46.8978	52.0242
30	5×5	15.2367	27.2228	36.5491	40.2398	28.9546	36.2782	46.6590	51.6819
35	6×6	15.2362	27.1962	36.5410	40.1419	28.9514	36.1474	46.1930	51.6707
40	7×7	15.2210	27.1960	36.4296	40.1296	28.9282	36.1463	46.1841	51.4184
40	8×8	15.2210	27.1960	36.4296	40.1296	28.9282	36.1463	46.1841	51.4184

4.2. Comparison Study

In order to validate the present method, Tables 4, 5 and 6 are devoted to compare the results obtained from this paper with published papers in the literature. Since no study has been reported on the free vibration of sandwich plate in contact with fluid, this section first compares dry natural frequencies of sandwich plate with the results presented in the literature. Then, the wet natural frequencies of isotropic plates are compared.

As a first comparison study, in Table 4, the dry natural frequencies of square sandwich plate with simply-supported boundary conditions are compared with the analytical solutions based on layer wise approach [22], the FEM solutions based on high-order shear deformations theory [53], and other analytical solutions based on high-order shear deformation theory and considering ESL approach[17, 18].

Table 4: Dimensionless dry natural frequencies ($\omega = \bar{\omega} a^2 \sqrt{\rho_c/E_c}\,/h$) for simply-supported sandwich plate with different lay-ups and $a/b = 1, a/h = 10$ and $h_c/h = 0.88$. (Lay-up 1: [0/90/0/Core/0/90/0] and Lay-up 2: [45/-45/45/Core/-45/45/-45])

Lay-ups	Mode No.	Method				
		Present	Analytical [22]	FEM-HSDT	Analytical-HSDT	FEM–HSDT

				(LW) [53]	(ESL) [17]	(ESL) [18]
Lay-up 1	ω_1	14.282	14.83	14.440	15.28	15.34
	ω_2	26.1842	26.91	26.826	28.69	30.18
	ω_3	26.8221	27.47	27.456	30.01	31.96
	ω_4	34.5165	35.57	35.706	38.86	40.94
Lay-up 2	ω_1	15.245	15.53	15.405	16.38	16.43
	ω_2	26.7295	27.36	27.417	29.65	31.17
	ω_3	26.7295	27.36	27.417	29.65	31.17
	ω_4	35.3905	36.93	36.592	40	42.78

The next comparison study is devoted to the dry natural frequencies of the sandwich plate with different boundary conditions. As shown in Table 5, the first six dimensionless dry natural frequencies of square sandwich plate are compared with various types of FEM models. The material properties M5 and M6 are used for the core and face sheets, respectively.

The FEM solution presented by Chalak et al. [52] is based on higher-order zig-zag model. Also, Kulkarni and Kapuria [54] reported the results based on zig-zag model for different boundary conditions along with the 3D results from ABAQUS software package.

Table 5: Dimensionless dry natural frequencies ($\omega = 100\bar{\omega}a\sqrt{\rho_c/E_t}$) for sandwich plate with lay-up [0/90/Core/90/0] and different boundary conditions (a/b=1, a/h=10, h_c/h=0.8)

B.C.	Method	Frequencies					
		ω_1	ω_2	ω_3	ω_4	ω_5	ω_6
CFCF	Present	7.0426	7.7690	14.2215	15.2980	17.1898	21.5046
	Chalak [52]	7.0359	7.7249	14.2105	15.2415	17.1179	21.3580
	3D Abaqus [54]	7.0119	7.7131	14.1496	15.1975	17.0942	21.3089
	ZIGT FE [54]	7.0923	7.8284	14.3407	15.4498	17.1776	21.5871
CFFF	Present	2.9740	3.6312	9.4107	10.7907	15.8589	17.2400
	Chalak [52]	2.9721	3.6053	9.3976	10.7219	15.8489	17.2203
	3D Abaqus [54]	2.9674	3.6113	9.3738	10.7228	15.8337	17.5148
	ZIGT FE [54]	2.9791	3.6348	9.4418	10.8109	15.8500	17.3072
CSCS	Present	10.3848	15.3560	18.2338	21.4893	21.6985	26.7959
	Chalak [52]	10.3027	16.1798	18.3228	22.1962	23.2839	27.1750
	3D Abaqus [54]	10.2816	16.1245	18.3029	22.1480	23.1797	27.1464
	ZIGT FE [54]	10.3582	16.3499	18.3744	22.4100	23.5983	27.2300
CCCC	Present	11.3166	16.8330	19.1758	23.0592	23.7886	28.4357
	Chalak [52]	11.2607	16.7446	19.0385	22.8018	23.6414	28.1930
	3D Abaqus [54]	11.2236	16.6777	18.9650	22.7096	23.5270	28.0728
	ZIGT FE [54]	11.4158	17.0329	19.3780	23.4305	24.0862	28.7241

Table 6 shows another comparison study, in which an isotropic plate coupled with a fluid is considered. The geometric and material properties of the plate are: $a = 10\ m, b = 10\ m, h = 0.15\ m, \rho = 2400\ \ kg/m^3, E = 25\ GPa$ and $v = 0.15$. Also, the width of the container and the mass density of the fluid are: $c = 100\ m$ and $\rho_f = 1000\ \ kg/m^3$. The results in this comparison have been obtained for different ratios of the fluid depth ($d/b =$ 0.2 ,0.4 ,0.6, 0.8 and 1). As can be seen from Tables 4, 5 and 6, there is an excellent agreement between the results from the present method and the available data in the literatures.

Table 6: Comparison study of the dimensionless natural frequencies ($\omega = \overline{\omega} a^2/\pi^2 \sqrt{12\rho_p(1-\ v^2)/Eh^2}$)of a square isotropic plate coupled with fluid

Mode	Method	d/b 0	0.2	0.4	0.6	0.8	1
(1,1)	Present	3.1394	3.0601	2.3419	1.6389	1.2819	1.1175
	Omiddezyani [33]	3.139	3.052	2.335	1.639	1.281	1.117
	Ugurlu [34]	3.169	3.064	2.196	1.496	1.173	1.036
	Khorshidi	3.1415	3.0127	2.0746	1.3563	1.0172	0.8565
(2,1)	Present	7.8403	7.2236	5.8004	4.4777	3.8798	3.2254
	Omiddezyani [33]	7.837	7.186	5.776	4.47	3.878	3.225
	Ugurlu [34]	7.902	7.092	5.708	5.174	3.926	3.337
	Khorshidi [30]	7.8527	6.9032	5.5313	4.9530	3.7329	3.1434
(1,2)	Present	7.8403	7.6369	5.9253	5.2698	3.8952	3.6883
	Omiddezyani [33]	7.837	7.609	5.919	5.265	3.899	3.687
	Ugurlu [34]	7.902	7.622	5.382	4.058	3.484	3.261
	Khorshidi [30]	7.8528	7.4957	5.0916	3.7884	3.2288	3.0037
(2,2)	Present	12.5981	11.6135	10.1930	8.9846	6.8847	5.8711
	Omiddezyani [33]	12.525	11.501	10.153	8.925	6.839	5.847
	Ugurlu [34]	12.68	11.40	9.974	8.746	6.777	5.942
	Khorshidi [30]	12.563	11.074	9.7556	8.4732	6.5952	5.6503
(3,1)	Present	15.6673	14.0444	11.6623	9.6395	8.7689	7.6436
	Omiddezyani [33]	15.644	13.938	11.47	9.594	8.731	7.562
	Ugurlu [34]	15.95	13.80	12.57	10.57	9.41	7.848
	Khorshidi [30]	15.6962	13.3586	12.1332	10.2708	9.1994	7.7808
(3,2)	Present	20.6552	18.6283	17.3675	14.8131	12.3494	10.6039
	Omiddezyani [33]	20.312	18.259	16.686	14.198	11.994	10.462
	Ugurlu [34]	20.69	18.10	16.68	14.47	12.66	10.72
	Khorshidi [30]	20.4023	17.6359	16.1027	14.1435	12.4425	10.9678
(2,3)	Present	20.6553	19.2150	17.9124	16.0522	13.0619	10.7520
	Omiddezyani [33]	20.312	18.721	17.544	14.907	12.355	10.661
	Ugurlu [34]	20.69	18.64	17.52	14.57	11.74	10.63
	Khorshidi [30]	20.4023	18.5549	17.3109	15.0785	12.2572	10.4765
(4,1)	Present	27.5749	24.8262	22.0406	18.6427	16.9125	14.8851

Omiddezyani [33]	26.519	23.971	19.677	17.248	16.113	14.384
Ugurlu [34]	27.52	24.21	21.36	19.32	17.66	14.91
Khorshidi [30]	26.6411	23.3108	20.53	18.6439	18.7913	15.6739

4.3. Parametric Studies

After validating the performance of the proposed formulation and approach, several numerical examples are employed in this section to study the vibrational characteristics of the sandwich plate with various boundary conditions contacting with fluid.

4.3.1. Effect of the presence of fluid on the natural frequencies

Table 7 demonstrates the first four dimensionless natural frequencies of sandwich plate with six different boundary conditions coupled with fluid. The material properties M1 and M2 are applied for the core and face sheets, respectively. As can be observed, the highest natural frequencies are related to fully clamped sandwich plate. On the contrary, the lowest natural frequencies are related to SSSF. Furthermore, it can be seen that by increasing the depth of fluid from 0 to 0.5, the natural frequency is reduced for all boundary conditions. It is worth mentioning that when one edge of the boundaries in sandwich plate is free (usually top edge), the effect of fluid on the fundamental natural frequencies is less than that edge of the boundary being simply-supported or clamped. This aspect is also seen later in the study of the effect of flexural modulus of the face sheet to that of the core.

Table 7: Dimensionless natural frequencies ($\omega = \bar{\omega} a^2 \sqrt{\rho_c/E_c}/h$) of square sandwich plate with various boundary conditions, Lay-up [0/90/0/Core/0/90/0] and $a/h = 10$, $a/b = 1$, $h_c/h = 0.88$

Depth of fluid	Mode No.	Boundary conditions					
		SSSS	CCCC	SSCF	CCCF	SSSF	CSCS
$\frac{d}{b} = 0$	ω_1	14.2820	17.9478	10.9319	13.6366	10.4886	16.1656
	ω_2	26.1842	28.3883	19.1317	20.2508	18.3217	27.5669
	ω_3	26.8221	28.8626	24.9796	26.3918	24.8432	27.6220
	ω_4	34.5165	36.7106	30.2877	31.4783	29.6955	35.8010
$\frac{d}{b} = 0.5$	ω_1	7.9622	9.6957	8.2467	9.5128	7.4852	8.8980
	ω_2	14.2809	15.3701	12.6052	14.4552	12.4461	14.6373
	ω_3	16.7998	18.3301	14.7364	15.6284	14.3003	17.7068
	ω_4	20.9687	21.9413	19.1831	20.1398	18.3529	21.1843

4.3.2. Effect of Side to Thickness Ratio (*a*/h) on the Wet Natural Frequency

Fig. 3 illustrates the fundamental wet natural frequencies of five layered square sandwich plate [0/90/Core/0/90] with $a/b = 1$, $c/a = 0.5$ and $f_C/f_t = 10$ in contact with different depths of fluid. It also contains different boundary conditions and varying side-to-thickness ratios. The material properties M3 and M4 are used for the core and face sheets, respectively.

As can be seen, by decreasing the side to thickness ratio (a/h), the natural frequencies decrease. This effect can be ascribed to the significant contribution of shear deformation and rotary inertia. Likewise, as the fluid depth increases, the natural frequencies decrease. Moreover, as stated earlier the highest natural frequencies are related to the fully clamped boundary conditions which are due to this fact that for this boundary condition, the general stiffness of the system is maximum. It should be noted that FSDT is deemed sufficient to predict the vibrational characteristics of moderately thick plates ($\frac{a}{h} \geq 10$). For the thick plates ($\frac{a}{h} \leq 10$), FSDT may produce unreliable results.

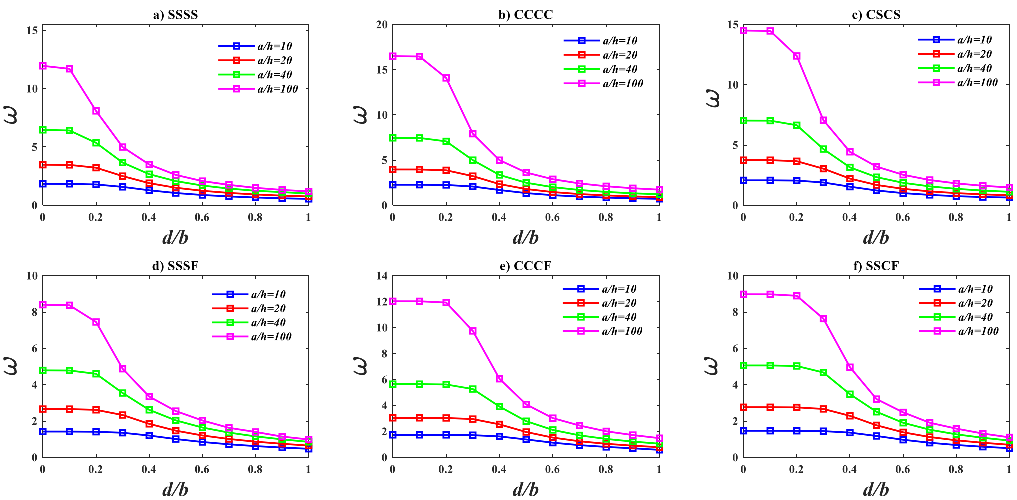

Fig. 3: Variation of dimensionless fundamental natural frequency of sandwich plate [0/90/Core/0/90] with different boundary conditions versus dimensionless depth of the fluid ($a/b = 1$, $c/a = 0.5$ and $f_c/f_t = 10$)

4.3.3. Effect of Flexural Modulus of the Face Sheet to the Core Ratio (E_t/E_C)

This section covers the influence of flexural modulus of the face sheet to flexural modulus of the core ratio on the natural frequencies. Fig. 4 presents fundamental wet and dry natural frequencies of sandwich plate with $a/h = 10$, $c/a = 0.5, d/b = 0.45$ and $f_c/h = 0.88$. It can be seen that the wet natural frequencies are always less than the dry ones. Furthermore, by increasing the ratio of flexural modulus of the face sheet to that of the core, both dry and wet natural frequencies increase. Moreover, when one edge of the sandwich plate is free, the difference between dry and wet natural frequencies is lower than when all edges are simply supported or clamped.

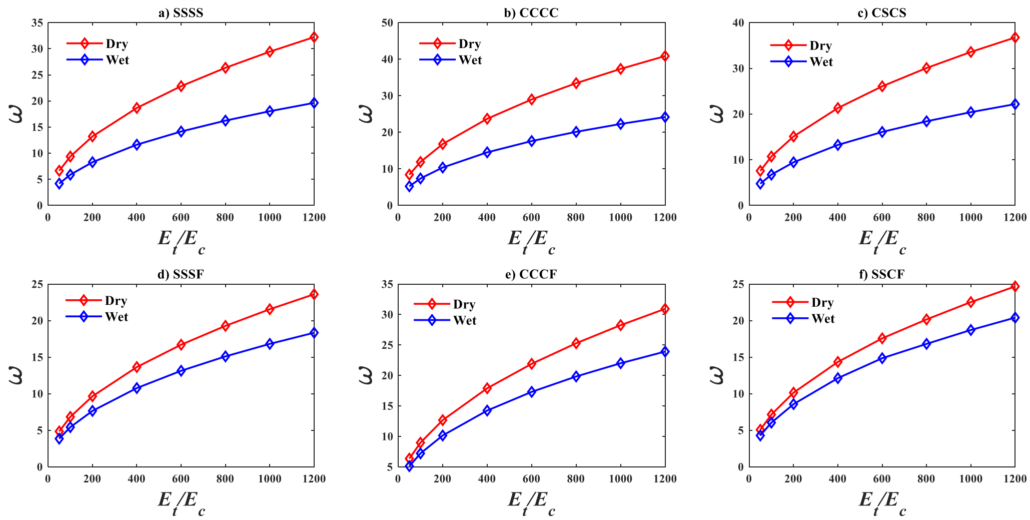

Fig. 4: Variation of dimensionless fundamental natural frequency of square sandwich plate [0/90/0/Core/0/90/0] with different boundary conditions coupled with fluid for various values of flexural modulus of the face sheet to that of the core.
$(a/h = 10, f_c/h = 0.88, d/b = 0.45, c/a = 0.5)$

4.3.4. Effect of Thickness of the Core to Thickness of the Face Sheet Ratio (f_c/f_t)

Fig. 5 shows the influence of thickness of the core to thickness of the face sheet ratio on the fundamental wet natural frequencies of square sandwich plate with lay-up [0/90/Core/0/90]. The material properties M3 and M4 from Table 1 are adopted for the core and face sheets, respectively. In this example, three different depths of the fluid ($d/b = 0.1, 0.3$ and 0.5) are considered. It is clear that the stiffness of the sandwich plate increases as the ratio of (f_c/f_t) increases. Therefore, the fundamental natural frequencies increase. Also, with increasing depth of fluid, the natural frequencies decrease. In addition, the boundary conditions listed in Fig. 5 follow the same trend as stated earlier. Also, the highest and lowest fundamental wet natural frequencies are related to the fully clamped boundary conditions and SSSF (three edges simply-supported and the other one free), respectively.

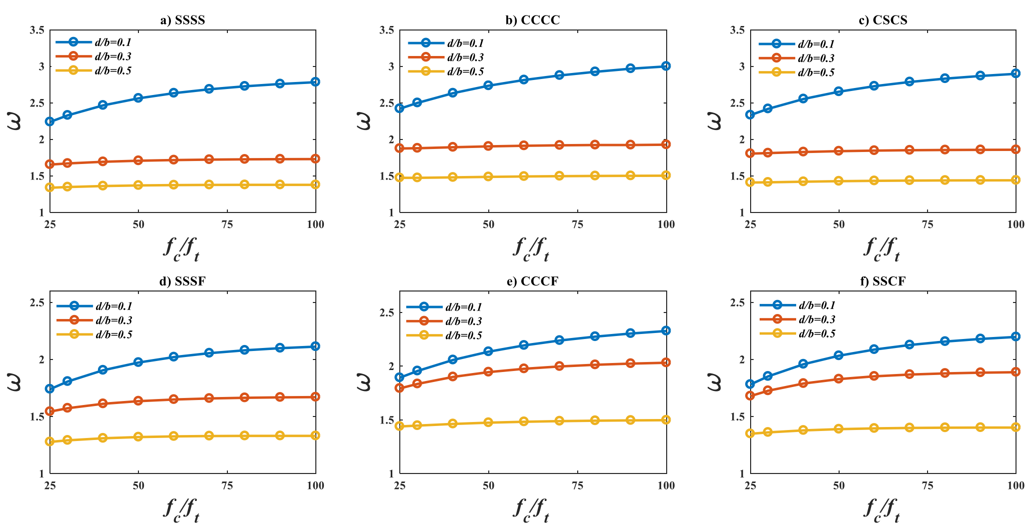

Fig. 5: Variation of dimensionless fundamental natural frequency of square sandwich plate [0/90/Core/0/90] with different boundary conditions in contact with fluid for various values of thickness of the core to thickness of the face sheet.
$(a/h = 10,\ a/b = 1,\ c/a = 0.5)$

4.3.5. Effect of Container Width Ratio on the Wet Natural Frequency

In Fig. 6, the numerical results are given for a seven layered square sandwich plate with lay-up [0/90/0/Core/0/90/0] and different container width ratio (c/a). The material properties M1 and M2 from Table 1 are chosen for the core and face sheets, respectively. Fig. 6 indicates as the width ratio of container increases, the fundamental natural frequencies increase for all boundary conditions shown in Fig. 6. It is worth mentioning that for high values of width ratio, changes in the fundamental natural frequencies are greatly reduced and tend to the specific value.

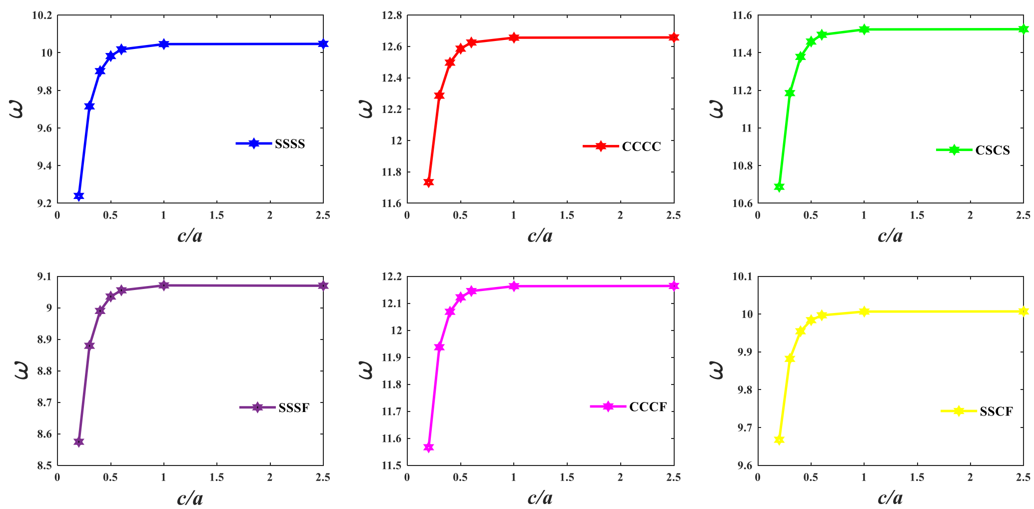

Fig. 6: Variation of dimensionless fundamental natural frequency of sandwich plate [0/90/0/Core/0/90/0] with different boundary conditions versus width of the container
$(a/b = 1,\ a/h = 10,\ d/b = 0.4$ and $f_c/h = 0.88)$

4.3.6. Effect of Sandwich Plate Aspect Ratio (a/b) on the Wet Natural Frequency

Fig. 7 presents the effect of plate aspect ratio (a/b) on the first dimensionless wet natural frequency of sandwich plate with lay-ups [45/-45/45/Core/-45/45/-45] and [0/90/0/Core/0/90/0] coupled with fluid. Results are given for dimensions $(a/h = 10, f_c/h = 0.88,\ d/b = 0.3$ and $c/a = 0.5)$ and two different boundary conditions just for brevity. Material properties M1 and M2 are chosen from Table 1 for the core and face sheets, respectively. It is found that fundamental natural frequencies illustrate an increasing trend up as the aspect ratio increases. In addition, comparison between two lay-ups reveals sandwich plate with lay-up [45/-45/45/Core/-45/45/-45] has higher natural frequencies than another one [0/90/0/Core/0/90/0]. In should be mentioned that another comparison between these two lay-ups has been done in Table 4 in which the environment is dry.

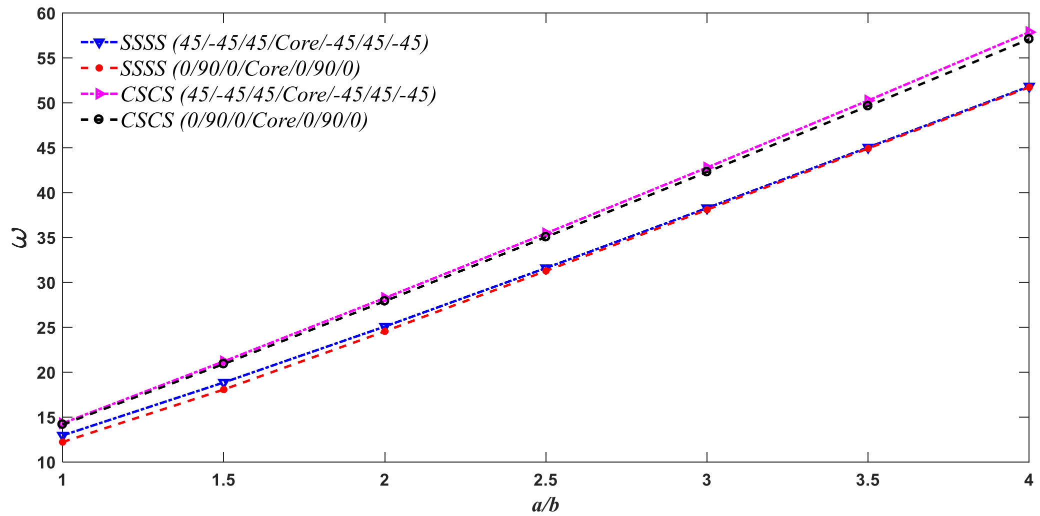

Fig. 7: Variation of dimensionless fundamental natural frequency of sandwich plate with two different lay-ups versus aspect ratio (a/b) for SSSS and CSCS boundary conditions in contact with fluid ($a/h = 10$, $f_c/h = 0.88, d/b = 0.3$ and $c/a = 0.5$)

4.3.7. Effect of Fluid Presence on the Wet Mode Shapes

In order to appreciate the effect of fluid on the fluid-structure interaction, the first six mode shapes of sandwich plate in contact with fluid are shown in Fig. 8. Also, for comparison purposes, the first six mode shapes of sandwich plate in air are presented in Fig. 9. As can be observed, the presence of fluid causes distortion in the mode shapes.

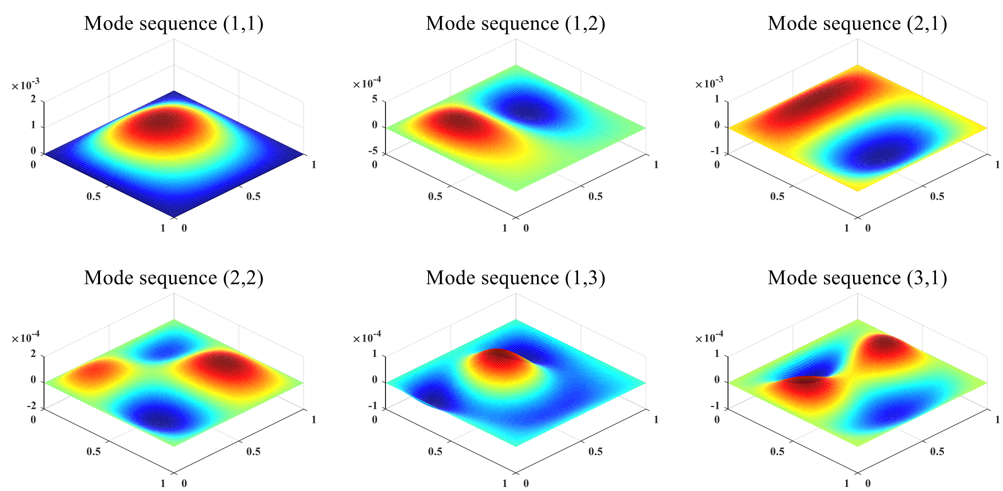

Fig. 8. First six mode shapes of a sandwich plate with lay-up [0/90/0/Core/0/90/0] and ($a/h = 10$, $f_c/h = 0.88$, $a/b = 1$) in contact with fluid ($d/b = 0.5$ and $c/a = 10$).

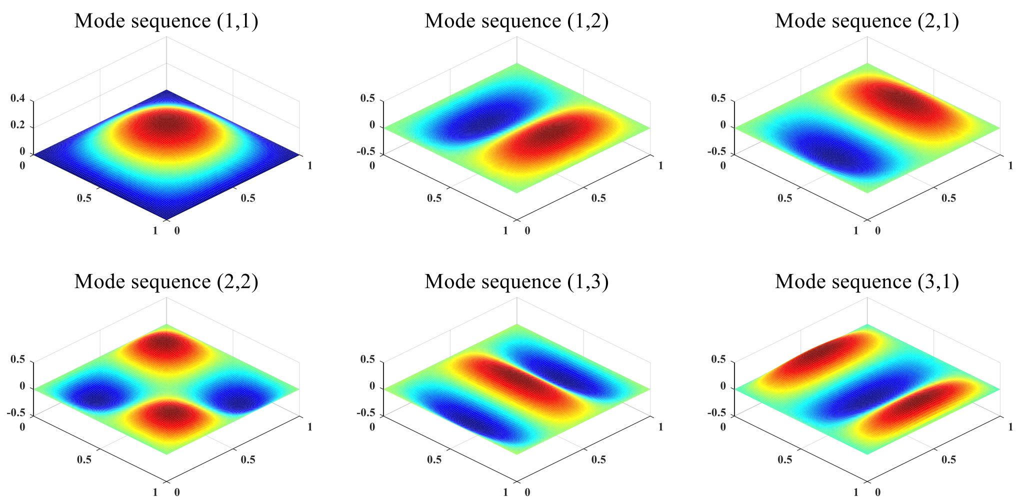

Fig. 9: First six mode shapes of a sandwich plate with lay-up (0/90/0/Core/0/90/0) and ($a/h = 10$, $f_c/h = 0.88$, $a/b = 1$) in air.

5. Conclusion

In this paper, the vibrational behavior of a sandwich plate with compressible core and different boundary conditions has been investigated where whether the top or bottom face sheet of sandwich plate has been coupled with fluid. The extended higher-order sandwich plate theory has been used for the analysis of sandwich plate in which both the in-plane and out of plane stresses of the core are considered. Also, the first-order shear deformation theory is adopted to the face sheets of sandwich plate. In additions assumptions for the fluid were also considered to be incompressible, Irrotational and inviscid. Hamilton's principle has been used to achieve governing differential equations of motions and corresponding boundary conditions. Rayleigh-Ritz method with two-variable orthogonal polynomials is used to solve the eigenvalue problem related to the free vibration of sandwich plate with various boundary conditions in contact with fluid. As presented in the numerical results section, wet natural frequencies are always lower than dry natural frequencies. In addition as the depth of fluid increases, the natural frequencies decrease for all types of boundary conditions. The fully clamped boundary conditions has the highest natural frequencies among all the examples are studied. Also with increasing the side to thickness ratio of the sandwich plate, the natural frequencies increase. It is observed that by increasing the thickness of the core to thickness of the face sheet, the natural frequencies increase. Furthermore the numerical results show that the natural frequencies increase as the aspect ratio increases. As the width of the tank increases, the natural frequencies increase and eventually tend to a certain amount. The distortion that the fluid has caused is shown in the mode shapes. For the future study, the free surface wave and also the compressibility of the fluid can be considered in the mathematical modeling.

6. Acknowledgement

The first and second authors acknowledge the funding support of Babol Noshirvani University of Technology through Grant program No. BNUT/964113035/97.

Appendix A

The governing equations and corresponding boundary conditions are derived as follows:
For the top face sheet:

$$\begin{aligned}
&N_{xx,x}^t + N_{xy,y}^t + \frac{2}{f_c^2} M_{2xx,x}^c + \frac{2}{f_c^2} M_{2xy,y}^c + \frac{4}{f_c^2} M_{Q1xz}^c + \frac{4}{f_c^3} M_{3xx,x}^c + \frac{4}{f_c^3} M_{3xy,y}^c \\
&\quad + \frac{12}{f_c^3} M_{Q2xz}^c - I_0^t u_{0,tt}^t - I_1^t \psi_{x,tt}^t - \frac{4}{f_c^3} I_3^c u_{0,tt} - \frac{2}{f_c^2} I_2^c u_{0,tt} \\
&\quad - \frac{4}{f_c^3} I_4^c u_{1,tt} - \frac{2}{f_c^2} I_3^c u_{1,tt} - \frac{4}{f_c^3} I_5^c u_{2,tt} - \frac{2}{f_c^2} I_4^c u_{2,tt} - \frac{4}{f_c^3} I_6^c u_{3,tt} \\
&\quad - \frac{2}{f_c^2} I_5^c u_{3,tt} = 0
\end{aligned} \tag{A-1}$$

$$\begin{aligned}
&N_{yy,y}^t + N_{xy,x}^t + \frac{2}{f_c^2} M_{2yy,y}^c + \frac{2}{f_c^2} M_{2xy,x}^c + \frac{4}{f_c^2} M_{Q1yz}^c + \frac{4}{f_c^3} M_{3yy,y}^c + \frac{4}{f_c^3} M_{3xy,x}^c \\
&\quad + \frac{12}{f_c^3} M_{Q2yz}^c - I_0^t v_{0,tt}^t - I_1^t \psi_{y,tt}^t - \frac{4}{f_c^3} I_3^c v_{0,tt} - \frac{2}{f_c^2} I_2^c v_{0,tt} \\
&\quad - \frac{4}{f_c^3} I_4^c v_{1,tt} - \frac{2}{f_c^2} I_3^c v_{1,tt} - \frac{4}{f_c^3} I_5^c v_{2,tt} - \frac{2}{f_c^2} I_4^c v_{2,tt} - \frac{4}{f_c^3} I_6^c v_{3,tt} \\
&\quad - \frac{2}{f_c^2} I_5^c v_{3,tt} = 0
\end{aligned} \tag{A-2}$$

$$\begin{aligned}
&Q_{xz,x}^t + Q_{yz,y}^t + \frac{1}{f_c} M_{Q1yz,y}^c + \frac{1}{f_c} M_{Q1xz,x}^c + \frac{1}{f_c} R_Z^c + \frac{2}{f_c^2} M_{Q2yz,y}^c + \frac{2}{f_c^2} M_{Q2xz,x}^c \\
&\quad + \frac{4}{f_c^2} M_Z^c - I_0^t w_{0,tt}^t - \frac{1}{f_c} I_1^c w_{0,tt} - \frac{2}{f_c^2} I_2^c w_{0,tt} - \frac{1}{f_c} I_2^c w_{1,tt} \\
&\quad - \frac{2}{f_c^2} I_3^c w_{1,tt} - \frac{1}{f_c} I_3^c w_{2,tt} - \frac{2}{f_c^2} I_4^c w_{2,tt} + \frac{1}{2} \rho_f (\dot{\Phi}_B + \dot{\Phi}_S) = 0
\end{aligned} \tag{A-3}$$

$$\begin{aligned}
&M_{xx,x}^t + M_{xy,y}^t + Q_{xz}^t - \frac{f_t}{f_c^2} M_{2xx,x}^c - \frac{f_t}{f_c^2} M_{2xy,y}^c - 2\frac{f_t}{f_c^2} M_{Q1xz}^c - 2\frac{f_t}{f_c^3} M_{3xx,x}^c \\
&\quad - 2\frac{f_t}{f_c^3} M_{3xy,y}^c - 6\frac{f_t}{f_c^3} M_{Q2xz}^c - I_1^t u_{0,tt}^t - I_2^t \psi_{x,tt}^t + 2\frac{f_t}{f_c^3} I_3^c u_{0,tt} \\
&\quad + \frac{f_t}{f_c^2} I_2^c u_{0,tt} + 2\frac{f_t}{f_c^3} I_4^c u_{1,tt} + \frac{f_t}{f_c^2} I_3^c u_{1,tt} + 2\frac{f_t}{f_c^3} I_5^c u_{2,tt} + \frac{f_t}{f_c^2} I_4^c u_{2,tt} \\
&\quad + 2\frac{f_t}{f_c^3} I_6^c u_{3,tt} + \frac{f_t}{f_c^2} I_5^c u_{3,tt} = 0
\end{aligned} \tag{A-4}$$

$$\begin{aligned}
&M_{yy,y}^t + M_{xy,x}^t + Q_{yz}^t - \frac{f_t}{f_c^2} M_{2yy,y}^c - \frac{f_t}{f_c^2} M_{2xy,x}^c - 2\frac{f_t}{f_c^2} M_{Q1yz}^c - 2\frac{f_t}{f_c^3} M_{3yy,y}^c \\
&\quad - 2\frac{f_t}{f_c^3} M_{3xy,x}^c - 6\frac{f_t}{f_c^3} M_{Q2yz}^c - I_1^t v_{0,tt}^t - I_2^t \psi_{y,tt}^t + 2\frac{f_t}{f_c^3} I_3^c v_{0,tt} \\
&\quad + \frac{f_t}{f_c^2} I_2^c v_{0,tt} + 2\frac{f_t}{f_c^3} I_4^c v_{1,tt} + \frac{f_t}{f_c^2} I_3^c v_{1,tt} + 2\frac{f_t}{f_c^3} I_5^c v_{2,tt} + \frac{f_t}{f_c^2} I_4^c v_{2,tt} \\
&\quad + 2\frac{f_t}{f_c^3} I_6^c v_{3,tt} + \frac{f_t}{f_c^2} I_5^c v_{3,tt} = 0
\end{aligned} \tag{A-5}$$

For the core:

$$N_{xx,x}^{c} + N_{xy,y}^{c} - \frac{4}{f_c^2} M_{2xx,x}^{c} - \frac{4}{f_c^2} M_{2xy,y}^{c} - \frac{8}{f_c^2} M_{Q1xz}^{c} - I_0^c u_{0,tt} + \frac{4}{f_c^2} I_2^c u_{0,tt} - I_1^c u_{1,tt} + \frac{4}{f_c^2} I_3^c u_{1,tt} - I_2^c u_{2,tt} + \frac{4}{f_c^2} I_4^c u_{2,tt} - I_3^c u_{3,tt} + \frac{4}{f_c^2} I_5^c u_{3,tt} = 0 \tag{A-6}$$

$$N_{yy,y}^{c} + N_{xy,x}^{c} - \frac{4}{f_c^2} M_{2yy,y}^{c} - \frac{4}{f_c^2} M_{2xy,x}^{c} - \frac{8}{f_c^2} M_{Q1yz}^{c} - I_0^c v_{0,tt} + \frac{4}{f_c^2} I_2^c v_{0,tt} - I_1^c v_{1,tt} + \frac{4}{f_c^2} I_3^c v_{1,tt} - I_2^c v_{2,tt} + \frac{4}{f_c^2} I_4^c v_{2,tt} - I_3^c v_{3,tt} + \frac{4}{f_c^2} I_5^c v_{3,tt} = 0 \tag{A-7}$$

$$Q_{yz,y}^{c} + Q_{xz,x}^{c} - \frac{4}{f_c^2} M_{Q2yz,y}^{c} - \frac{4}{f_c^2} M_{Q2xz,x}^{c} - \frac{8}{f_c^2} M_{z}^{c} - I_0^c w_{0,tt} + \frac{4}{f_c^2} I_2^c w_{0,tt} - I_1^c w_{1,tt} + \frac{4}{f_c^2} I_3^c w_{1,tt} - I_2^c w_{2,tt} + \frac{4}{f_c^2} I_4^c w_{2,tt} = 0 \tag{A-8}$$

$$M_{yy.y}^{c} + M_{xy.x}^{c} + Q_{yz}^{c} - \frac{4}{f_c^2} M_{3yy,y}^{c} - \frac{4}{f_c^2} M_{3xy,x}^{c} - \frac{12}{f_c^2} M_{Q2yz}^{c} - I_1^c v_{0,tt} + \frac{4}{f_c^2} I_3^c v_{0,tt} - I_2^c v_{1,tt} + \frac{4}{f_c^2} I_4^c v_{1,tt} - I_3^c v_{2,tt} + \frac{4}{f_c^2} I_5^c v_{2,tt} - I_4^c v_{3,tt} + \frac{4}{f_c^2} I_6^c v_{3,tt} = 0 \tag{A-9}$$

$$M_{xx,x}^{c} + M_{xy,y}^{c} + Q_{xz}^{c} - \frac{4}{f_c^2} M_{3xx,x}^{c} - \frac{4}{f_c^2} M_{3xy,y}^{c} - \frac{12}{f_c^2} M_{Q2xz}^{c} - I_1^c u_{0,tt} + \frac{4}{f_c^2} I_3^c u_{0,tt} - I_2^c u_{1,tt} + \frac{4}{f_c^2} I_4^c u_{1,tt} - I_3^c u_{2,tt} + \frac{4}{f_c^2} I_5^c u_{2,tt} - I_4^c u_{3,tt} + \frac{4}{f_c^2} I_6^c u_{3,tt} = 0 \tag{A-10}$$

For bottom face sheet:

$$N_{xx,x}^{b} + N_{xy,y}^{b} + \frac{2}{f_c^2} M_{2xx,x}^{c} + \frac{2}{f_c^2} M_{2xy,y}^{c} + \frac{4}{f_c^2} M_{Q1xz}^{c} - \frac{4}{f_c^3} M_{3xx,x}^{c} - \frac{4}{f_c^3} M_{3xy,y}^{c} - \frac{12}{f_c^3} M_{Q2xz}^{c} - I_0^b u_{0,tt}^b - I_1^b \psi_{x,tt}^b + \frac{4}{f_c^3} I_3^c u_{0,tt} - \frac{2}{f_c^2} I_2^c u_{0,tt} + \frac{4}{f_c^3} I_4^c u_{1,tt} - \frac{2}{f_c^2} I_3^c u_{1,tt} + \frac{4}{f_c^3} I_5^c u_{2,tt} - \frac{2}{f_c^2} I_4^c u_{2,tt} + \frac{4}{f_c^3} I_6^c u_{3,tt} - \frac{2}{f_c^2} I_5^c u_{3,tt} = 0 \tag{A-11}$$

$$
\begin{aligned}
&N_{yy,y}^{b}+N_{xy,x}^{b}+\frac{2}{f_c^2}M_{2yy,y}^{c}+\frac{2}{f_c^2}M_{2xy,x}^{c}+\frac{4}{f_c^2}M_{Q1yz}^{c}+\frac{4}{f_c^3}M_{3yy,y}^{c}-\frac{4}{f_c^3}M_{3xy,x}^{c}\\
&\qquad-\frac{12}{f_c^3}M_{Q2yz}^{c}-I_0^b v_{0,tt}^{b}-I_1^b\psi_{y,tt}^{b}+\frac{4}{f_c^3}I_3^c v_{0,tt}-\frac{2}{f_c^2}I_2^c v_{0,tt}\\
&\qquad+\frac{4}{f_c^3}I_4^c v_{1,tt}-\frac{2}{f_c^2}I_3^c v_{1,tt}+\frac{4}{f_c^3}I_5^c v_{2,tt}-\frac{2}{f_c^2}I_4^c v_{2,tt}+\frac{4}{f_c^3}I_6^c v_{3,tt}\\
&\qquad-\frac{2}{f_c^2}I_5^c v_{3,tt}=0
\end{aligned}
\tag{A-12}
$$

$$
\begin{aligned}
&Q_{xz,x}^{b}+Q_{yz,y}^{b}-\frac{1}{f_c}M_{Q1yz,y}^{c}-\frac{1}{f_c}M_{Q1xz,x}^{c}-\frac{1}{f_c}R_Z^c+\frac{2}{f_c^2}M_{Q2yz,y}^{c}+\frac{2}{f_c^2}M_{Q2xz,x}^{c}\\
&\qquad+\frac{4}{f_c^2}M_z^c-I_0^b w_{0,tt}^{b}+\frac{1}{f_c}I_1^c w_{0,tt}-\frac{2}{f_c^2}I_2^c w_{0,tt}+\frac{1}{f_c}I_2^c w_{1,tt}\\
&\qquad-\frac{2}{f_c^2}I_3^c w_{1,tt}+\frac{1}{f_c}I_3^c w_{2,tt}-\frac{2}{f_c^2}I_4^c w_{2,tt}=0
\end{aligned}
\tag{A-13}
$$

$$
\begin{aligned}
&M_{xx,x}^{b}+M_{xy,y}^{b}+Q_{xz}^{b}+\frac{f_b}{f_c^2}M_{2xx,x}^{c}+\frac{f_b}{f_c^2}M_{2xy,y}^{c}+2\frac{f_b}{f_c^2}M_{Q1xz}^{c}-2\frac{f_b}{f_c^3}M_{3xx,x}^{c}\\
&\qquad-2\frac{f_b}{f_c^3}M_{3xy,y}^{c}-6\frac{f_b}{f_c^3}M_{Q2xz}^{c}-I_1^b u_{0,tt}^{b}-I_2^b\psi_{x,tt}^{b}+2\frac{f_b}{f_c^3}I_3^c u_{0,tt}\\
&\qquad-\frac{f_b}{f_c^2}I_2^c u_{0,tt}+2\frac{f_b}{f_c^3}I_4^c u_{1,tt}-\frac{f_b}{f_c^2}I_3^c u_{1,tt}+2\frac{f_b}{f_c^3}I_5^c u_{2,tt}-\frac{f_b}{f_c^2}I_4^c u_{2,tt}\\
&\qquad+2\frac{f_b}{f_c^3}I_6^c u_{3,tt}-\frac{f_b}{f_c^2}I_5^c u_{3,tt}=0
\end{aligned}
\tag{A-14}
$$

$$
\begin{aligned}
&M_{yy,y}^{b}+M_{xy,x}^{b}+Q_{yz}^{b}+\frac{f_b}{f_c^2}M_{2yy,y}^{c}+\frac{f_b}{f_c^2}M_{2xy,x}^{c}+2\frac{f_b}{f_c^2}M_{Q1yz}^{c}-2\frac{f_b}{f_c^3}M_{3yy,y}^{c}\\
&\qquad-2\frac{f_b}{f_c^3}M_{3xy,x}^{c}-6\frac{f_v}{f_c^3}M_{Q2yz}^{c}-I_1^t v_{0,tt}^{t}-I_2^t\psi_{y.tt}^{t}+2\frac{f_b}{f_c^3}I_3^c v_{0,tt}\\
&\qquad-\frac{f_b}{f_c^2}I_2^c v_{0,tt}+2\frac{f_b}{f_c^3}I_4^c v_{1,tt}-\frac{f_b}{f_c^2}I_3^c v_{1,tt}+2\frac{f_b}{f_c^3}I_5^c v_{2,tt}-\frac{f_b}{f_c^2}I_4^c v_{2,tt}\\
&\qquad+2\frac{f_b}{f_c^3}I_6^c v_{3,tt}-\frac{f_b}{f_c^2}I_5^c v_{3,tt}=0
\end{aligned}
\tag{A-15}
$$

Furthermore, the corresponding boundary conditions are given as follows:
At $x=0$ and $x=a$:

$$
\begin{aligned}
&N_{xx}^{i}=0\ or\ u_0^i=0\ ;\ M_{xx}^{i}=0\ or\ \psi_x^i=0\ ;\ N_{xy}^{i}=0\ or\ v_0^i=0\\
&M_{xy}^{i}=0\ or\ \psi_y^i=0\ ;\ Q_{xz}^{i}=0\ or\ w_0^i=0\ ;\ M_{Q1xz}^{i}=0\ or\ w_1=0\\
&M_{xz}^{i}=0\ or\ w_2=0\ ;\ Q_{xz}^{c}=0\ or\ w_0=0\ ;\ N_{xx}^{c}=0\ or\ u_0=0\\
&M_{xx}^{c}=0\ or\ u_1=0\ ;\ M_{2xx}^{c}=0\ or\ u_2=0\ ;\ M_{3xx}^{c}=0\ or\ u_3=0\\
&N_{xy}^{c}=0\ or\ v_0=0\ ;\ M_{xy}^{c}=0\ or\ v_1=0\ ;\ M_{2xy}^{c}=0\ or\ v_2=0\\
&M_{3xy}^{c}=0\ or\ v_3=0
\end{aligned}
\tag{B}
$$

At $y=0$ and $y=a$:

$$
\begin{aligned}
&N_{yy}^{i}=0\ or\ v_0^i=0\ ;\ M_{yy}^{i}=0\ or\ \psi_y^i=0\ ;\ N_{xy}^{i}=0\ or\ u_0^i=0\ ;\\
&M_{xy}^{i}=0\ or\ \psi_y^i=0\ ;\ Q_{yz}^{i}=0\ or\ w_0^i=0\ ;\ M_{Q1yz}^{c}=0\ or\ w_1=0\ ;\\
&M_{Q2yz}^{c}=0\ or\ w_2=0\ ;\ Q_{yz}^{c}=0\ or\ w_0=0\ ;\ N_{xy}^{c}=0\ or\ u_0=0\ ;
\end{aligned}
\tag{C}
$$

$M_{xy}^c = 0 \ or \ u_1 = 0$; $M_{2xy}^c = 0 \ or \ u_2 = 0$; $M_{3xy}^c = 0 \ or \ u_3 = 0$;
$N_{yy}^c = 0 \ or \ v_0 = 0$; $M_{yy}^c = 0 \ or \ v_1 = 0$; $M_{2yy}^c = 0 \ or \ v_2 = 0$;
$M_{3yy}^c = 0 \ or \ v_3 = 0$;

Appendix B

Generally, the basic functions ($\lambda_i^k(k = w^t, w^b, w^c, \dots, u_1{}^c)$) can be considered as follows:

a)

$$\lambda_1^{w^l} = x^\gamma y^\gamma (x-a)^\gamma (y-b)^\gamma \quad \text{(D-1)}$$

in which $l = t, b, c$ and:

$$\gamma = \begin{cases} 0 & \text{if edge is free} \\ 1 & \text{if edge is simply} - \text{suppoted} \\ 2 & \text{if edge is clamped} \end{cases}$$

b)

$$\lambda_1^{u^l} = x^\beta y^\beta (x-a)^\beta (y-b)^\beta \quad \text{(D-2)}$$

and:

$$\lambda_1^{u^l} = \lambda_1^{x^k} = \lambda_1^{u_1{}^c} \quad \text{(D-3)}$$

where $l = t, b, c, \quad k = t, b$ and:

$$\beta = \begin{cases} 0 & \text{if edge is free or simply} - \text{suported in } y - \text{direction} \\ 1 & \text{if edge is simply} - \text{suported in } x - \text{direction or clamped} \end{cases}$$

c)

$$\lambda_1^{v^l} = x^\xi y^\xi (x-a)^\xi (y-b)^\xi \quad \text{(D-4)}$$

and:

$$\lambda_1^{v^l} = \lambda_1^{y^k} = \lambda_1^{v_1{}^c} \quad \text{(D-5)}$$

where $l = t, b, c, \quad k = t, b$ and:

$$\xi = \begin{cases} 0 & \text{if edge is free or simply} - \text{suported in } x - \text{direction} \\ 1 & \text{if edge is simply} - \text{suported in } y - \text{direction or clamped} \end{cases}$$

References

[1] Li D, Deng Z, Xiao H, Jin P. Bending analysis of sandwich plates with different face sheet materials and functionally graded soft core. Thin-Walled Structures. 2018;122:8-16.

[2] Sharma N, Mahapatra TR, Panda SK. Hygrothermal effect on vibroacoustic behaviour of higher-order sandwich panel structure with laminated composite face sheets. Engineering Structures. 2019;197:109355.

[3] Shahgholian-Ghahfarokhi D, Aghaei-Ruzbahani M, Rahimi G. Vibration correlation technique for the buckling load prediction of composite sandwich plates with iso-grid cores. Thin-Walled Structures. 2019;142:392-404.

[4] Ahmadi SA, Pashaei M-H, Jafari-Talookolaei R-A. Three-dimensional elastic-plastic pulse response and energy absorption of curved composite sandwich panel using DQ–Newmark method. Engineering Structures. 2019;189:111-28.
[5] Dorduncu M. Stress analysis of sandwich plates with functionally graded cores using peridynamic differential operator and refined zigzag theory. Thin-Walled Structures. 2020;146:106468.
[6] Singha TD, Rout M, Bandyopadhyay T, Karmakar A. Free vibration analysis of rotating pretwisted composite sandwich conical shells with multiple debonding in hygrothermal environment. Engineering Structures. 2020;204:110058.
[7] Wang Y-j, Zhang Z-j, Xue X-m, Zhang L. Free vibration analysis of composite sandwich panels with hierarchical honeycomb sandwich core. Thin-Walled Structures. 2019;145:106425.
[8] Pagano NJ. Exact solutions for rectangular bidirectional composites and sandwich plates. Journal of composite materials. 1970;4:20-34.
[9] Noor AK, Peters JM, Burton WS. Three-dimensional solutions for initially stressed structural sandwiches. Journal of engineering mechanics. 1994;120:284-303.
[10] Srinivas S, Rao AK, Rao CJ. Flexure of simply supported thick homogeneous and laminated rectangular plates. ZAMM-Journal of Applied Mathematics and Mechanics/Zeitschrift für Angewandte Mathematik und Mechanik. 1969;49:449-58.
[11] Srinivas S, Rao CJ, Rao A. An exact analysis for vibration of simply-supported homogeneous and laminated thick rectangular plates. Journal of sound and vibration. 1970;12:187-99.
[12] Srinivas S, Rao A. Bending, vibration and buckling of simply supported thick orthotropic rectangular plates and laminates. International Journal of Solids and Structures. 1970;6:1463-81.
[13] Kant T. A higher-order theory for free vibration of unsymmetrically laminated composite and sandwich plates—finite element evaluations. Computers & structures. 1989;32:1125-32.
[14] Kant T, Swaminathan K. Analytical solutions for free vibration of laminated composite and sandwich plates based on a higher-order refined theory. Composite structures. 2001;53:73-85.
[15] Swaminathan K, Patil S, Nataraja M, Mahabaleswara K. Bending of sandwich plates with anti-symmetric angle-ply face sheets–Analytical evaluation of higher order refined computational models. Composite structures. 2006;75:114-20.
[16] Swaminathan K, Patil S. Analytical solutions using a higher order refined computational model with 12 degrees of freedom for the free vibration analysis of antisymmetric angle-ply plates. Composite structures. 2008;82:209-16.
[17] Meunier M, Shenoi R. Dynamic analysis of composite sandwich plates with damping modelled using high-order shear deformation theory. Composite structures. 2001;54:243-54.
[18] Nayak AK, Moy S, Shenoi R. Free vibration analysis of composite sandwich plates based on Reddy's higher-order theory. Composites Part B: Engineering. 2002;33:505-19.
[19] Bardell N, Dunsdon J, Langley R. Free vibration analysis of coplanar sandwich panels. Composite structures. 1997;38:463-75.
[20] Rao MK, Desai Y. Analytical solutions for vibrations of laminated and sandwich plates using mixed theory. Composite structures. 2004;63:361-73.
[21] Frostig Y, Thomsen OT. High-order free vibration of sandwich panels with a flexible core. International Journal of Solids and Structures. 2004;41:1697-724.
[22] Malekzadeh K, Khalili M, Mittal R. Local and global damped vibrations of plates with a viscoelastic soft flexible core: an improved high-order approach. Journal of Sandwich Structures & Materials. 2005;7:431-56.
[23] Malekzadeh K, Sayyidmousavi A. Free vibration analysis of sandwich plates with a uniformly distributed attached mass, flexible core, and different boundary conditions. Journal of Sandwich Structures & Materials. 2010;12:709-32.
[24] Khalili S, Mohammadi Y. Free vibration analysis of sandwich plates with functionally graded face sheets and temperature-dependent material properties: A new approach. European Journal of Mechanics-A/Solids. 2012;35:61-74.

[25] Singh S, Harsha S. Nonlinear dynamic analysis of sandwich S-FGM plate resting on pasternak foundation under thermal environment. European Journal of Mechanics-A/Solids. 2019;76:155-79.
[26] Sayyad AS, Ghugal YM. On the free vibration analysis of laminated composite and sandwich plates: A review of recent literature with some numerical results. Composite structures. 2015;129:177-201.
[27] Zhou D, Cheung Y. Vibration of vertical rectangular plate in contact with water on one side. Earthquake engineering & structural dynamics. 2000;29:693-710.
[28] Ergin A, Uğurlu B. Linear vibration analysis of cantilever plates partially submerged in fluid. Journal of Fluids and Structures. 2003;17:927-39.
[29] Chang T-P, Liu M-F. On the natural frequency of a rectangular isotropic plate in contact with fluid. Journal of Sound Vibration. 2000;236:547-53.
[30] Khorshid K, Farhadi S. Free vibration analysis of a laminated composite rectangular plate in contact with a bounded fluid. Composite structures. 2013;104:176-86.
[31] Cheung Y, Zhou D. Coupled vibratory characteristics of a rectangular container bottom plate. Journal of Fluids and Structures. 2000;14:339-57.
[32] Cheung Y, Zhou D. Hydroelastic vibration of a circular container bottom plate using the Galerkin method. Journal of Fluids and Structures. 2002;16:561-80.
[33] Omiddezyani S, Jafari-Talookolaei R-A, Abedi M, Afrasiab H. The size-dependent free vibration analysis of a rectangular Mindlin microplate coupled with fluid. Ocean Engineering. 2018;163:617-29.
[34] Uğurlu B, Kutlu A, Ergin A, Omurtag M. Dynamics of a rectangular plate resting on an elastic foundation and partially in contact with a quiescent fluid. Journal of sound and vibration. 2008;317:308-28.
[35] Hashemi SH, Karimi M, Taher HRD. Vibration analysis of rectangular Mindlin plates on elastic foundations and vertically in contact with stationary fluid by the Ritz method. Ocean Engineering. 2010;37:174-85.
[36] Eshaghi M. The effect of magnetorheological fluid and aerodynamic damping on the flutter boundaries of MR fluid sandwich plates in supersonic airflow. European Journal of Mechanics-A/Solids. 2020:103997.
[37] Zhou D, Liu W. Hydroelastic vibrations of flexible rectangular tanks partially filled with liquid. International Journal for Numerical Methods in Engineering. 2007;71:149-74.
[38] Rezvani SS, Kiasat MS. Analytical and experimental investigation on the free vibration of a floating composite sandwich plate having viscoelastic core. Archives of Civil and Mechanical Engineering. 2018;18:1241-58.
[39] Watts G, Pradyumna S, Singha M. Free vibration analysis of non-rectangular plates in contact with bounded fluid using element free Galerkin method. Ocean Engineering. 2018;160:438-48.
[40] Rahmani O, Khalili S, Malekzadeh K. Free vibration response of composite sandwich cylindrical shell with flexible core. Composite structures. 2010;92:1269-81.
[41] Chow S, Liew K, Lam K. Transverse vibration of symmetrically laminated rectangular composite plates. Composite structures. 1992;20:213-26.
[42] Bhat R. Flexural vibration of polygonal plates using characteristic orthogonal polynomials in two variables. Journal of sound and vibration. 1987;114:65-71.
[43] Liew K, Lam K, Chow S. Free vibration analysis of rectangular plates using orthogonal plate function. Computers & structures. 1990;34:79-85.
[44] Kumar Y. The Rayleigh–Ritz method for linear dynamic, static and buckling behavior of beams, shells and plates: a literature review. Journal of Vibration and Control. 2018;24:1205-27.
[45] Moreno-García P, dos Santos JVA, Lopes H. A review and study on Ritz method admissible functions with emphasis on buckling and free vibration of isotropic and anisotropic beams and plates. Archives of Computational Methods in Engineering. 2018;25:785-815.
[46] Chakraverty S, Bhat R, Stiharu I. Recent research on vibration of structures using boundary characteristic orthogonal polynomials in the Rayleigh-Ritz method. Shock and vibration digest. 1999;31:187-94.

[47] Nallim LG, Martinez SO, Grossi RO. Statical and dynamical behaviour of thin fibre reinforced composite laminates with different shapes. Computer methods in applied mechanics and engineering. 2005;194:1797-822.
[48] Moradi A, Ahmadikia H. Analytical solution for different profiles of fin with temperature-dependent thermal conductivity. Mathematical Problems in Engineering. 2010;2010.
[49] Frostig Y, Thomsen OT. On the free vibration of sandwich panels with a transversely flexible and temperature-dependent core material–Part I: Mathematical formulation. Composites Science and Technology. 2009;69:856-62.
[50] Yang C, Jin G, Ye X, Liu Z. A modified Fourier–Ritz solution for vibration and damping analysis of sandwich plates with viscoelastic and functionally graded materials. International Journal of Mechanical Sciences. 2016;106:1-18.
[51] Amabili M. Eigenvalue problems for vibrating structures coupled with quiescent fluids with free surface. Journal of sound and vibration. 2000;231:79-97.
[52] Chalak H, Chakrabarti A, Iqbal M, Sheikh AH. Free vibration analysis of laminated soft core sandwich plates. Journal of Vibration and Acoustics. 2013;135.
[53] Belarbi M-O, Tati A, Ounis H, Khechai A. On the Free Vibration Analysis of Laminated Composite and Sandwich Plates: A Layerwise Finite Element Formulation. Latin American Journal of Solids and Structures. 2017;14:2265-90.
[54] Kulkarni S, Kapuria S. Free vibration analysis of composite and sandwich plates using an improved discrete Kirchhoff quadrilateral element based on third-order zigzag theory. Computational Mechanics. 2008;42:803-24.